Manuscript prepared for J. Name
with version 4.2 of the LaTeX class copernicus.cls.
Date: 23 January 2015

Dust aerosol radiative effects during summer 2012 simulated with a coupled regional aerosol-atmosphere-ocean model over the Mediterranean

P. Nabat[1], S. Somot[1], M. Mallet[2], M. Michou[1], F. Sevault[1], F. Driouech[3], D. Meloni[4], A. di Sarra[4], C. Di Biagio[5], P. Formenti[5], M. Sicard[6], J.-F. Léon[2], and M.-N. Bouin[7]

[1]Météo-France, CNRM-GAME, Centre National de Recherches Météorologiques, UMR3589, Toulouse, France
[2]Laboratoire d'Aérologie, Toulouse, France
[3]Direction de la Météorologie Nationale du Maroc
[4]Laboratory for Earth Observations and Analyses, ENEA, Rome, Italy
[5]Laboratoire Interuniversitaire des Systèmes Atmosphériques (LISA), UMR7583 – CNRS, Créteil, France
[6]Universitat Politechnica de Catalunya, Barcelona, Spain
[7]Météo-France, CMM, Centre de Météorologie Marine, Brest, France

Abstract. The present study investigates the radiative ~~and climatic~~ effects of dust aerosols in the Mediterranean region during summer 2012 using a fully ~~coupled regional climate system model~~ (CNRM-RCSM5). A prognostic aerosol scheme, including desert dust, sea salt, organic, black-carbon and sulphate particles, has been integrated to CNRM-RCSM5, in addition to the atmosphere, land surface and ocean components. An evaluation of this aerosol scheme of CNRM-RCSM5, and especially of the dust aerosols, has been performed against in-situ and satellite measurements, showing its ability to reproduce the spatial and temporal variability of aerosol optical depth (AOD) over the Mediterranean region in summer 2012. Observations from the TRAQA/ChArMEx campaign also show that the model correctly represents dust vertical and size distributions. Three simulations have been carried out for summer 2012 with CNRM-RCSM5, including either the full prognostic aerosol scheme, only monthly-averaged AOD means from the aerosol scheme or no aerosols at all, in order to focus on the radiative ~~and climatic~~ effects of dust particles and the role of the prognostic scheme. Surface shortwave aerosol radiative forcing variability is found to be more than twice higher over regions affected by dust aerosols, when using a prognostic aerosol scheme instead of monthly AOD means. In this case downward surface solar radiation is also found to be better reproduced according to a comparison with several stations across the Mediterranean. A composite study over 14 stations across the Mediterranean, designed to identify days with high dust AOD, also reveals the improvement of the representation of surface temperature brought by the use of the prognostic aerosol scheme. Indeed the surface receives less radiation during dusty days, but only the simulation using the prognostic aerosol scheme is found to reproduce the observed intensity of the dimming and warming on dusty days. Moreover, the radiation and temperature averages over summer 2012 are also modified by the use of prognostic aerosols, mainly because of the differences brought in shortwave aerosol radiative forcing variability. Therefore this first comparison over summer 2012 highlights the importance of the choice of the representation of aerosols in climate models.

Correspondence to: P. Nabat
(pierre.nabat@meteo.fr)

1 Introduction

Numerous and various aerosols affect the Mediterranean basin (Lelieveld et al., 2002), located at the crossroads of air masses carrying both natural (desertic particles, sea-salt, volcanic ashes, etc.) and anthropogenic (black carbon, sulphate, etc.) particles. Because of their microphysical and optical properties, these aerosols can have strong effects on the regional radiative budget (e.g. Bergamo et al., 2008), with ensuing impact on climate (Zanis et al., 2012; Spyrou et al., 2013; Nabat et al., 2014), and ecosystems of the Mediterranean (Guieu et al., 2010). Among these aerosols, the Saharan desert dust particles represent an important contribution of aerosols for this region (Barnaba and Gobbi, 2004; Nabat et al., 2013). Indeed, dust particles coming from suspension, saltation and creeping processes associated with wind erosion (Knippertz and Todd, 2012), can move from northern Africa to the Mediterranean Sea and Europe (Moulin et al., 1997; Papadimas et al., 2008; Gkikas et al., 2013). These dust outbreaks are mainly driven by the synoptic meteorological conditions (Gkikas et al., 2012): they are more frequent in the eastern basin in winter and spring, in the central basin in spring and in the western basin in summer (Moulin et al., 1998). The ChArMEx initiative (Chemistry-Aerosol Mediterranean Experiment, http://charmex.lsce.ipsl.fr) has been launched for a few years in the framework of the MISTRALS (Mediterranean Integrated STudies at Regional And Local Scales) program, in order to improve our knowledge

of aerosols and their impacts on climate in the Mediterranean. Thus, in early summer 2012, the ChArMEx/TRAQA (TRansport and Air QuAlity) campaign focused on the characterization of the polluted air masses over the Mediterranean basin through the study of representative case studies. A particularly intense dust event has been measured at the end of June with different observation means (balloons, aircraft, surface and remote-sensing measurements), and consequently represents a documented case to evaluate the ability of regional climate models to reproduce this kind of events and the associated radiative and climatic effects of aerosols. Indeed the evaluation of regional climate models is possible through case studies, made possible by the use of a reanalysis as lateral boundary forcing which provides the real chronology of these events.

The aim of the present work is consequently to evaluate the direct and semi-direct effects of dust particles during summer 2012 both at the daily time scale and at the summer scale. We consider here a modelling approach, with the following requirements. First of all, in order to simulate dust outbreaks, models need prognostic dust schemes (emission, transport, deposition) to uplift dust particles from arid areas and transport them in the atmosphere. Many climate models indeed use only monthly aerosol climatology (e.g. Tanré et al., 1984; Tegen et al., 1997) that cannot correspond to this kind of study. However, let alone the chemistry-transport models (e.g. CHIMERE, MOCAGE) that do not have aerosol-climate interactions, several aerosol schemes already exist in different climate models (e.g. MACC, ECHAM-HAM, IPSL), evaluated in different intercomparison exercises (e.g., AEROCOM, Schulz et al., 2006, ACCMIP, Lamarque et al., 2013). With regards to dust aerosols, most of the climate models can simulate the main patterns of dust emission and transport (Woodage et al., 2010), but large uncertainties remain in the characterization of dust properties and the resulting impact on climate (Huneeus et al., 2011; Mahowald et al., 2013), notably because of differences in dust emission parameterizations (Todd et al., 2008). Over the Euro-Mediterranean region, several studies have considered the effects of aerosols on climate using simulations with a prognostic scheme, both for anthropogenic aerosols (Zanis, 2009; Vogel et al., 2009; Meier et al., 2012) and dust particles (Santese et al., 2010; Spyrou et al., 2013).

Moreover, the role of the Mediterranean Sea is essential in climate feedbacks (Somot et al., 2008; Artale et al., 2010; Herrmann et al., 2011), so that ocean-atmosphere coupled regional models have recently been developed (Krzic et al., 2011; Herrmann et al., 2011; Mariotti and Dell'Aquila, 2012; L'Hévéder et al., 2012; Turuncoglu et al., 2013; Nabat et al., 2014). The importance of this coupling in the aerosol-climate interactions in the Mediterranean has even been recently highlighted (Nabat et al., 2014). However, up to now, aerosol-climate studies with prognostic aerosol schemes have been achieved either with the COSMO (Vogel et al., 2009) or with the RegCM model (Giorgi et al., 2012), and have not included an ocean-atmosphere coupling yet, even if an ocean-atmosphere coupling is currently developed between RegCM and ROMS (Turuncoglu et al., 2013).

In addition, as the Mediterranean is also characterized by local winds, complex coastlines and orography, high resolution modelling is needed to correctly reproduce the atmospheric circulation (Gibelin and Déqué, 2003; Gao et al., 2006; Giorgi and Lionello, 2008).

From our knowledge, none of these regional models can have at the same time ocean-atmosphere coupling and prognostic aerosol schemes. In the present study, a new version of the coupled regional climate model system (RCSM) of the CNRM, called CNRM-RCSM5, has been developed, including an aerosol prognostic scheme derived from the GEMS/MACC project (Morcrette et al., 2009; Michou et al., 2014), in addition to the atmosphere, ocean and land-surface components. This new model tool thus complies with all the criteria mentioned above, and should be able to help us to evaluate the direct and semi-direct effects of dust aerosols at the daily time scale. The data brought by the TRAQA campaign provide the opportunity to a first evaluation of the dust aerosol scheme before assessing the radiative and climatic aerosol effects. Besides, including the other aerosol species allows a comparison of total aerosol optical depth with remote-sensing measurements. Thus the present work aims at studying the radiative and climatic effects of dust aerosols in the Mediterranean area during summer 2012. The question of the difference between the use of climatological and prognostic aerosols in this model will also be raised, notably to study the consequences of this choice both on the daily and seasonal (for summer) variability of different meteorological parameters (radiation, temperature, cloud cover).

After a description of the aerosol scheme in Sect. 2 and its evaluation in Sect. 3, the radiative and climatic effects of aerosols are studied in Sect. 4, before the concluding remarks in Sect. 5.

2 Methodology

2.1 The CNRM-RCSM5 model

Four different components are included in this regional climate model system: the atmosphere with the regional climate model ALADIN-Climate (Déqué and Somot, 2008; Colin et al., 2010), the ocean with the regional model NEMOMED8 (Beuvier et al., 2010), the land-surface with the model ISBA (Noilhan and Mahfouf, 1996) and the aerosols, simulated interactively within ALADIN-Climate (see details in 2.2). ALADIN-Climate is a bi-spectral semi-implicit semi-lagrangian regional model, with a 50 km horizontal resolution and 31 vertical levels in the present work. The version 5.3 is used here bringing some improvements compared to the previous version 5.2 used in Nabat et al. (2014). As in the version used in Lucas-Picher et al. (2013),

the longwave (LW) radiation scheme is now based on the Rapid Radiation Transfer Model (RRTM, Mlawer et al., 1997), while the shortwave (SW) scheme initially developed by Morcrette (1989) has a finer spectral resolution (6 bands). We also use here a spectral nudging method described in Radu et al. (2008), that enables us to keep large scales from the boundary forcing and thus impose the true natural climate variability which is essential to represent dust events notably. Here the wind vorticity and divergence, the surface pressure, the temperature and the specific humidity are nudged. The function used imposes a constant rate above 700 hPa, a relaxation zone between 700 and 850 hPa, while the levels below 850 hPa are free. The spatial wavelengths are similarly nudged beyond 400 km, with a relaxation zone between 200 and 400 km. Thus this method gives the model enough freedom to generate the aerosols at the surface while keeping the large scales conditions that are essential to simulate the true chronology.

The ocean model NEMOMED8 and the land surface model ISBA are the same models as used in Nabat et al. (2014). The ocean-atmosphere coupling is achieved by the OASIS3 coupler (Valcke, 2013) at a 3-hour frequency, which represents an improvement compared to CNRM-RCSM4 described in Nabat et al. (2014). Note finally that contrary to CNRM-RCSM4, the coupling to the river routine scheme is not included in the present version of CNRM-RCSM5.

2.2 The aerosol scheme in ALADIN-Climate

Until the version 5.2 of ALADIN-Climate aerosols were represented in this model through monthly climatologies of aerosol optical depth (AOD) for five aerosol types (desert dust, sea-salt, black carbon, organic matter and sulphate) distributed vertically according to constant profiles. In the version 5.3 used here, a prognostic aerosol scheme has been included, adapted from the GEMS/MACC aerosol scheme (Morcrette et al., 2009; Benedetti et al., 2011; Michou et al., 2014). It includes the same five aerosol species that can be directly emitted from the surface for dust and sea-salt particles, or from external emission datasets for black carbon, organic matter and sulphate precursors. The spatial domain of our simulations has consequently been extended compared to the previous study of Nabat et al. (2014), in order to include all the sources generating aerosols that can be transported over the Mediterranean basin. As far as dust particles are concerned (Middleton and Goudie, 2001; Israelevich et al., 2012), the following sources are notably included in the domain: North African sources (Morocco, Algeria, Tunisia), the Hoggar mountains, the Tibesti Mountains, the Bodele depression, Libya, Egypt as well as sources near the Red Sea (northeast Sudan, Djibouti). No aerosol is indeed included in the lateral boundary forcing.

Sea salt aerosols are generated by wind stress on ocean surface, either because of air bubbles bursting at the sea surface, or from spume droplets directly torn off the wave crests by the wind. Guelle et al. (2001) have reviewed different approaches to model these processes. The current formulation used in ALADIN-Climate is based on the studies of Guelle et al. (2001) and Schulz et al. (2004), that provide surface mass fluxes at 80% relative humidity depending on 10m-wind, integrated for the three size bins defined in the scheme: 0.03 to 0.5μm, 0.5 to 5μm and 5 to 20μm. Note that the size distribution of emitted sea salt also depends on other factors such as the sea surface temperature (Jaeglé et al., 2011), which are not taken into account in this current version.

Dust emission processes depend on several factors such as soil characteristics (chemical composition, humidity, roughness) and surface wind speed. In the GEMS/MACC scheme, the dust parameterization follows Ginoux et al. (2001), that propose a simplified formulation of dust emission, based on the wind speed and thresholds according to the fraction of bare soil and soil moisture. In ALADIN-Climate, this function has been replaced by the Marticorena and Bergametti (1995) parameterization, that takes into account more soil characteristics coming from the ECOCLIMAP database (Masson et al., 2003), which provides information on the erodible fraction and the sand and clay fractions, allowing a classification of the soil textures. After the determination of an erosion threshold based on the soil distribution, the soil moisture and the roughness caused by nonerodible elements, the horizontal saltation flux is calculated, proportionally to the third power of the wind friction velocity. The vertical flux is then inferred from this saltation flux, according to an empirical relationship given by Marticorena and Bergametti (1995), which notably depends on the soil clay content. The emitted dust size distribution is based on the work of Kok (2011). More details about this dust emission parameterization can be found in Nabat et al. (2012), who have used the same dust emission scheme in RegCM4. Once emitted dust particles are integrated in the three dust size bins of the scheme: 0.01 to 1.0μm, 1.0 to 2.5μm and 2.5 to 20μm.

The external emission datasets for the three other aerosol types come from Lamarque et al. (2010), who have provided inventories at 0.5°resolution of different species for climate models. These inventories include numerous sectors such as energy production, industries, domestic activities, agriculture, transport and fires. Organic and black carbon particles are separated between hydrophile and hydrophobic particles. SO_2 emitted particles can be transformed in SO_4, but 5% of them are directly emitted as SO_4 aerosols (Benkovitz et al., 1996). Volcanic sulfur emissions are also included, as well as DMS particles from oceans (see Michou et al., 2014).

All these aerosols gathered in 12 bins are then transported in the atmosphere, before possible dry or wet deposition. More details about transport and deposition can be found in Morcrette et al. (2009). Optical properties (single scattering albedo and asymmetry factor) are fixed for each aerosol type, as defined in Nabat et al. (2013). The complexity of this aerosol scheme is similar to the one used in RegCM, but it does not include detailed chemical processes that can be

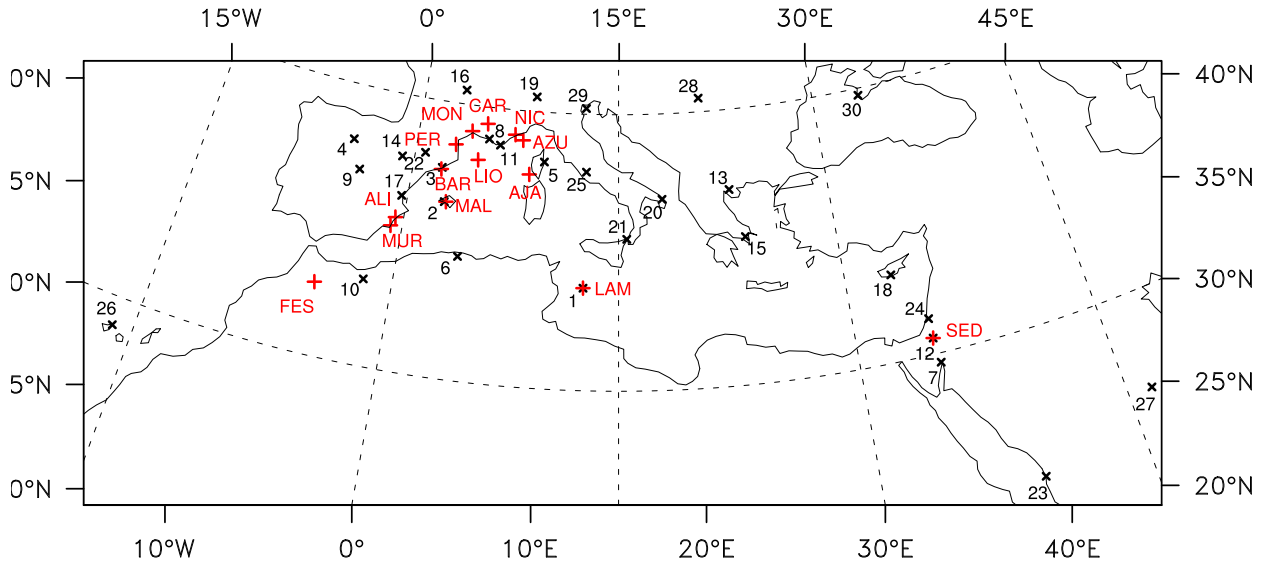

Fig. 1. Stations of the AERONET network (black crosses, see the list of the corresponding numbers in Figure 4). Red crosses indicate the stations providing measurements of surface radiation and temperature (see the list in Table 1).

found in COSMO-ART (Vogel et al., 2009). However it enables our model to keep a low cost of calculations, so that multi-annual simulations could be carried out for aerosol-climate studies. Note also that nitrate aerosols are not considered in this model.

2.3 Simulations

Three simulations have been carried out with CNRM-RCSM5, driven by the ERA-Interim reanalysis (Dee et al., 2011) as initial and lateral boundary forcing. First of all, the PROG simulation includes the whole aerosol prognostic scheme described previously. Secondly, in order to estimate the effect of aerosols on meteorological variables such as temperature and radiation, a simulation without aerosols is needed: the NO simulation does not include any aerosols. Thirdly, as the objective of this study is also to discuss the choice of using climatological or prognostic aerosols, another simulation, called PROG-M, uses monthly AOD provided by PROG, so that PROG and PROG-M share the same average aerosol content at the monthly scale. Comparisons between these simulations will enable us to estimate the aerosol effects on the radiative budget and regional climate, and the implications of using a prognostic aerosol scheme instead of monthly climatologies. While an improvement on daily SW radiation variability is expected with the use of prognostic aerosols, it is more difficult to answer a priori for other daily parameters (2m-temperature, SST), and more generally for consequences on the summer average. The three simulations cover the summer 2012 period from 1st June to 31st August. A one-month spin-up period has been performed for each simulation in order to have realist aerosol concentrations on 1st June.

2.4 Observation data

For the evaluation of the aerosols and their direct radiative effects, different observed datasets are used in the present work.

Simulated AOD is compared to satellite data from the MODerate resolution Imaging Spectroradiometer (MODIS, collection 5.1, standard and Deep Blue algorithms, 1°resolution, Tanré et al., 1997; Levy et al., 2007), the Multiangle Imaging SpectroRadiometer (MISR, Level3, Kahn et al., 2005, 2010) and the SEVIRI radiometer onboard the geostationary satellite Meteosat Second Generation (MSG). For the latter instrument, we use the algorithm of Carrer et al. (2010), which provides high-resolution AOD over both ocean and land surfaces. Nowadays, this algorithm is being implemented on the production chain of the ICARE thematic center (http://www.icare.univ-lille1.fr) under the name of AERUS-GEO (Aerosol and surface albEdo Retrieval Using a directional Splitting method - application to GEO data Carrer et al., 2014) which is a daytime averaged product.

Ground-based observations from 30 stations of the AErosol RObotic NETwork (AERONET, Holben et al., 1998, 2001) will also be considered (Figure 1). These sun-photometer observations provide high-quality data (Level 2.0), which have been downloaded from the AERONET website (http://aeronet.gsfc.nasa.gov). All AOD data have been calculated at 550 nm using the Angstrom coefficient when necessary, to make comparisons and evaluation easier.

Short name	Station	Lat	Lon	Available days	Dusty days
MUR	Murcia	37.8	-0.8	83	23
BAR	Barcelona	41.3	2.1	85	10
MAL	Palma de Mallorca	39.6	2.6	74	13
ALI	Alicante	38.3	-0.6	90	15
AJA	Ajaccio	41.6	8.5	88	7
CAR	Carpentras	44.1	5.1	84	4
MON	Montpellier	43.6	4.0	75	7
NIC	Nice	43.7	7.2	88	4
PER	Perpignan	42.7	2.9	80	6
FES	Fès	33.9	-5.0	61	36
LIO	Gulf of Lions (buoy)	42.1	4.6	83	9
AZU	Azur (buoy)	43.4	7.8	78	5
LAM	Lampedusa	35.5	12.6	89	24
SED	Sede-Boker	30.9	34.8	92	5

Table 1. Stations used for the composite study. The total number of days when observations are available and among them the number of dusty days have been indicated.

The TRAQA campaign has also provided interesting observations for dust aerosols, namely vertical profiles from lidar instruments in Barcelona and San Giuliano (Corsica). The Barcelona lidar system is part of the ACTRIS/EARLINET network (Aerosols, Clouds, and Trace gases Research InfraStructure Network / European Aerosol Research Lidar Network, Pappalardo et al., 2014). The extinction coefficient profiles were retrieved by means of the two-component elastic lidar inversion algorithm constrained with the AERONET sun-photometer-derived AOD (Reba et al., 2010). In San Giuliano (42.28°N, 9.51°E), aerosol vertical profiles were acquired with a 355 nm backscattering lidar. The aerosol extinction coefficient profiles are estimated using the Klett's method and a fixed lidar ratio (Léon et al., this issue, in prep.) from hourly averaged attenuated range-corred lidar signals. Besides, an ATR-42 research flight operated by SAFIRE (Service des Avions Francais Instrumentés pour la Recherche en Environnement) has also been realized during the TRAQA campaign. This study uses the airborne data from the Passive Cavity Aerosol Spectrometer Probe (PCASP), which measures particles between 0.1 and 3.2 μm.

In addition, the Météo-France and AEMET networks have provided daily radiation and 2m-temperature measurements (see Figure 1 and Table 1). Radiation measurements have been completed by the stations of Sede-Boker (SED, SolRad-Net network, AERONET website), Lampedusa (LAM, coll. ENEA) and two Météo-France buoys located in the Gulf of Lions (LIO) and near the French Riviera (AZU). Lampedusa and the two buoys also provide sea surface temperature (SST) measurements. All the fourteen stations providing surface radiation and temperature have been added in Figure 1 (red crosses). It is worth mentioning that available data is provided by stations that are located for most of them in the western Mediterranean. However, in summer, most of the dust outbreaks occur in this region because of frequent low pressure systems over Morocco that favour the dust export over the western Mediterranean (Moulin et al., 1998; Gkikas et al., 2012).

Datasets	MODIS	MISR	AERUS-GEO	MACC
CNRM-RCSM5	0.64	0.77	0.65	0.74
MODIS		0.81	0.69	0.84
MISR			0.68	0.84
AERUS-GEO				0.61

Table 2. Spatial correlation coefficients between AOD of the different datasets presented in Figure 2

Besides, the MACC reanalysis (Morcrette et al., 2009) is also used in the present work, as a means of evaluating the CNRM-RCSM5 simulations. This reanalysis includes data assimilation of AOD from the MODIS instrument.

3 Evaluation of the simulated aerosols

In this section, an evaluation of the simulated aerosols during summer 2012 is carried out against different available observations and climatologies. Depending on the parameter, several types of datasets are indeed required.

3.1 Total AOD: spatial evaluation

The AOD spatial distribution is firstly evaluated against different satellite products (MODIS, MISR and AERUS-GEO). The average total AOD in summer 2012 for each dataset is shown in Figure 2. The general spatial pattern shows a good agreement between satellites and CNRM-RCSM5. The highest values (up to 1.5) are indeed found over northern Africa and Arabian peninsula while the Mediterranean Sea is affected by moderate AOD, ranging from 0.15 to 0.3, from the north-east to the south-west.

In greater detail, some differences can be noted between the model and satellite data. CNRM-RCSM5 AOD is closer to MISR over northern Africa, where a large zone of AOD higher than 0.5 can be identified in both datasets, while

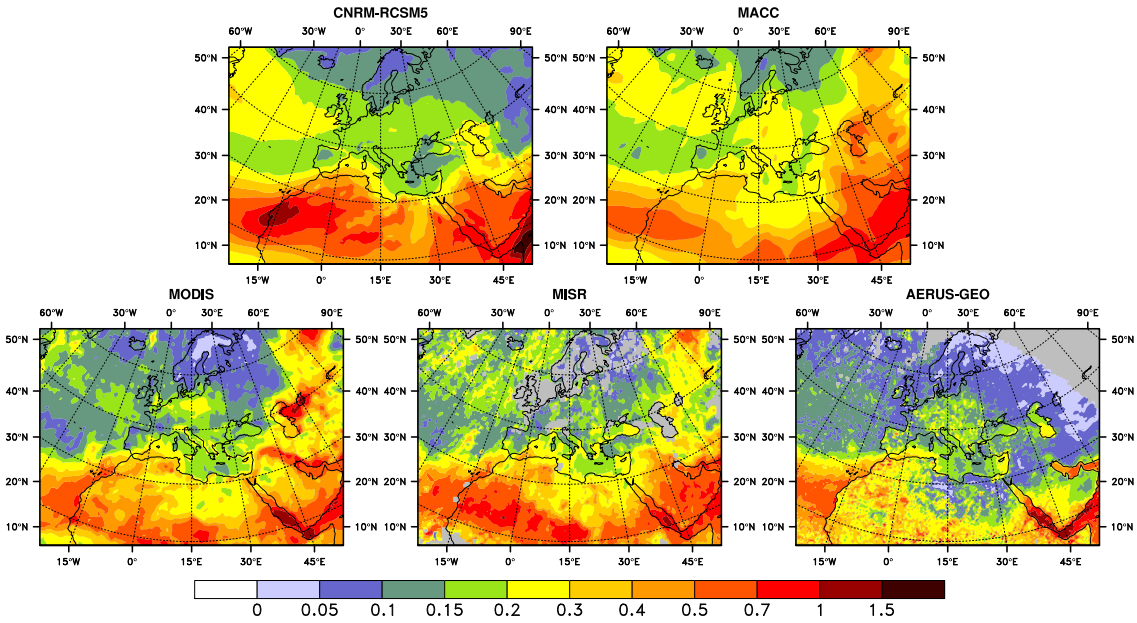

Fig. 2. Mean aerosol optical depth at 550 nm in summer 2012 (JJA) simulated by CNRM-RCSM5 and MACC (top), and measured by 3 satellite instruments (MODIS, MISR and AERUS-GEO, bottom)

MODIS and especially AERUS-GEO show lower AOD. Similar conclusions can be drawn for the Arabian peninsula. Dust export over the Atlantic ocean is on the contrary in very good agreement between the five products (AOD between 0.5 and 0.7). Over western and central Europe, MISR AOD is lower than MODIS, AERUS-GEO and CNRM-RCSM5. Large differences in AOD are also present in Eastern Europe and Russia, where MODIS shows higher AOD than the other datasets. However, this region is in the limit of the domain seen by SEVIRI (lower values in AERUS-GEO), and is also close to the border of the domain used in CNRM-RCSM5, so that aerosols over this region may come from outside the domain. Finally, AOD over the northern Atlantic ocean is higher in CNRM-RCSM5 than in satellite products, but the presence of numerous clouds in this area limits the quality of the satellite data there.

In summary, Table 2 presents the spatial correlations between these four products. All the correlations are higher than 0.6, confirming the general agreement, and the ability of CNRM-RCSM5 to reproduce the main spatial patterns of AOD.

3.2 Total AOD: temporal evaluation

As far as the temporal dimension is concerned, an evalution has been realized against ground-based measurements from the AERONET network in the Mediterranean area in terms of daily means. Indeed AERONET measurements benefit from a higher temporal resolution than data from moving satellites and their accuracy is generally higher, about ± 0.01 (Holben et al., 1998) against about ± 0.05 for satellites (Kahn et al., 2010; Levy et al., 2010). Figure 3 shows four temporal series across the Mediterranean basin, respectively at Oujda (a, Morocco, number 10 in Figure 1), Mallorca (b, Spain, 2), Frioul (c, France, 8) and Lampedusa (d, Italy, 1). All these series show high daily variability, because of frequent dust outbreaks in this season. The spectral nudging technique used in CNRM-RCSM5 enables the model to reproduce the true chronology of the synoptic meteorological conditions as shown in Herrmann et al. (2011), which is useful for driving dust emission. in the present work. As a result, the model is able to reproduce the intensity and the chronology of most AOD peaks, such as those observed in Oujda (18th June, 25th July) in Mallorca (19th June, 9th July, 10th August), Frioul (28th June, 19th August) and Lampedusa (21st June, 13th August). However, CNRM-RCSM5 overestimate a few dust events (e.g. 19th June in Frioul, 15th June in Lampedusa), but these differences remain in minority.

Similar comparisons have been realized for 30 AERONET stations (see their locations on Figure 1), the results are presented in a Taylor diagram (Figure 4, adapted to daily time series from Taylor, 2001). This diagram represents three statistics: the correlation coefficient is the azimuth angle, the radial distance from the origin is the standard deviation normalised by observations, and the distance to the "REF" point on the x-axis is the root-mean-square error (RMSE). The average temporal correlation coefficient for CNRM-RCSM5 is 0.70, while the ratio between simulated and observed standard deviations is 1.01, revealing the ability of the aerosol scheme to reproduce AOD daily variability. In addition, CNRM-RCSM5 has no station with very low scores, and has a low mean bias both when considering all the 30 stations

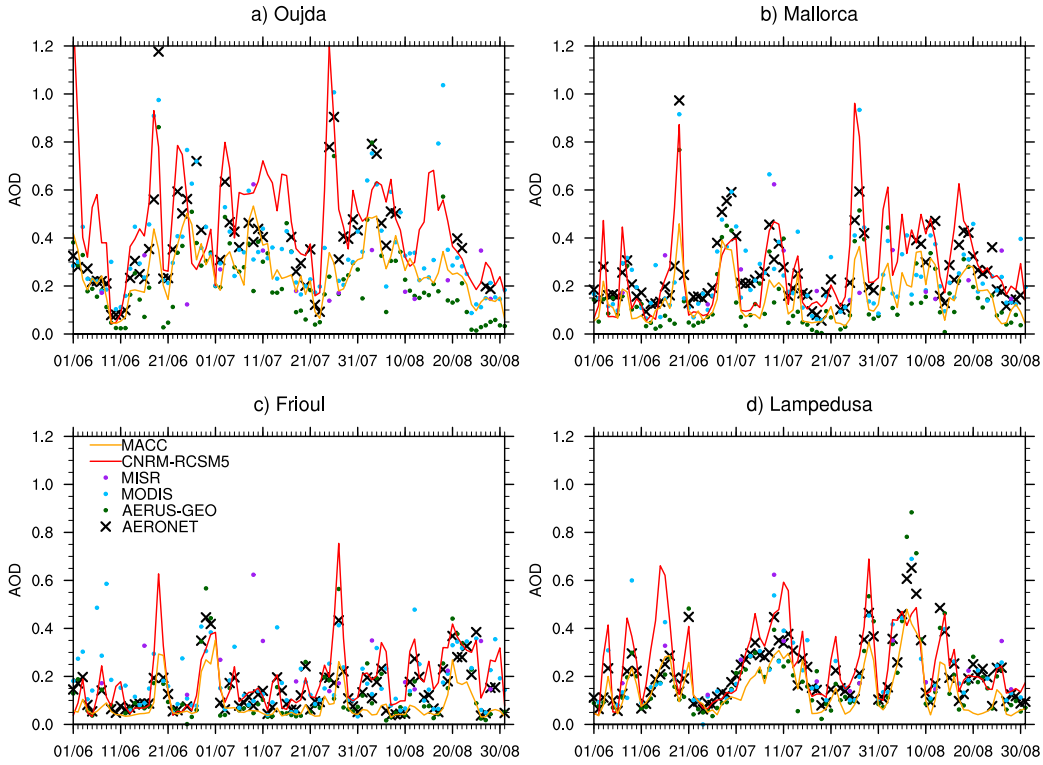

Fig. 3. AOD (at 550 nm) temporal series between 1st June and 31st August 2012 simulated by CNRM-RCSM5 (red lines) and MACC (orange lines), and observed by AERONET sunphotometers (black crosses), MODIS (blue crosses) and AERUS-GEO (green crosses), at four stations of the AERONET network: Oujda (a, number 10 in Figure 1), Mallorca (b, 2), Frioul (c, 8) and Lampedusa (d, 1).

(0.02) and only the stations to the south of 33°N (0.03).

Besides, the daily values for the satellite products have been added in Figures 3 and 4 as information for data users. It is indeed important to note that in terms of daily variability, (1) MODIS and AERUS-GEO have a higher temporal correlation with AERONET (resp. 0.73 and 0.76) than MISR (0.15), probably because of a reduced number of available retrievals with this instrument, (2) AERUS-GEO has the best scores among the satellite products, (3) MODIS and AERUS-GEO have however respectively 5 and 3 stations with RMSE higher than 1.25, and (4) all these products have a higher mean bias than CNRM-RCSM5.

3.3 Contribution of aerosol species to AOD

Satellites and ground-based measurements do not provide the contribution of the different aerosol types to AOD (the distinction between coarse and fine modes is not sufficient), that is the reason why a comparison to the MACC reanalysis (Morcrette et al., 2009; Benedetti et al., 2011) and the AOD climatology from Nabat et al. (2013), named NAB13 thereafter, is presented in this section. Note that total AOD of NAB13 corresponds to MODIS AOD by definition of this product, and that the total AOD of MACC has been added in Figures 2, 3 and 4, and Table 2 as information for data users.

Figure 5 presents the mean AOD for summer 2012 for the five simulated aerosol types. Dust aerosols prevail in the southern part of the domain because of sources in Sahara and in the Arabian peninsula, while anthropogenic particles, especially sulphate and organic matter, are responsible for local maxima in AOD in Europe. Sea-salt particles are essentially simulated over the Atlantic ocean, as well as the western Mediterranean Sea in lower quantities.

The different contributions to AOD for each aerosol type are given in Table 3, for CNRM-RCSM5, MACC and NAB13. NAB13 and MACC are based on both model and satellite data for the first one, and on model and data assimilation for the second one. NAB13, which gives reliable estimations of the different AOD components, is only available on the 2003-2009 period, so that the average over this period with the minimum and maximum values have been indicated. Averages have been calculated on the three domains defined in Nabat et al. (2013): Europe, the Mediterranean Sea and northern Africa.

Over Europe, CNRM-RCSM5 is very close to NAB13 for total AOD (0.18 on average) and the five aerosol types, even if the sharing between organic matter and sulphate aerosols is slightly different. MACC simulate more dust and sulphate particles, but the three satellite data have lower AOD (between 0.15 and 0.16), so that CNRM-RCSM5 AOD is

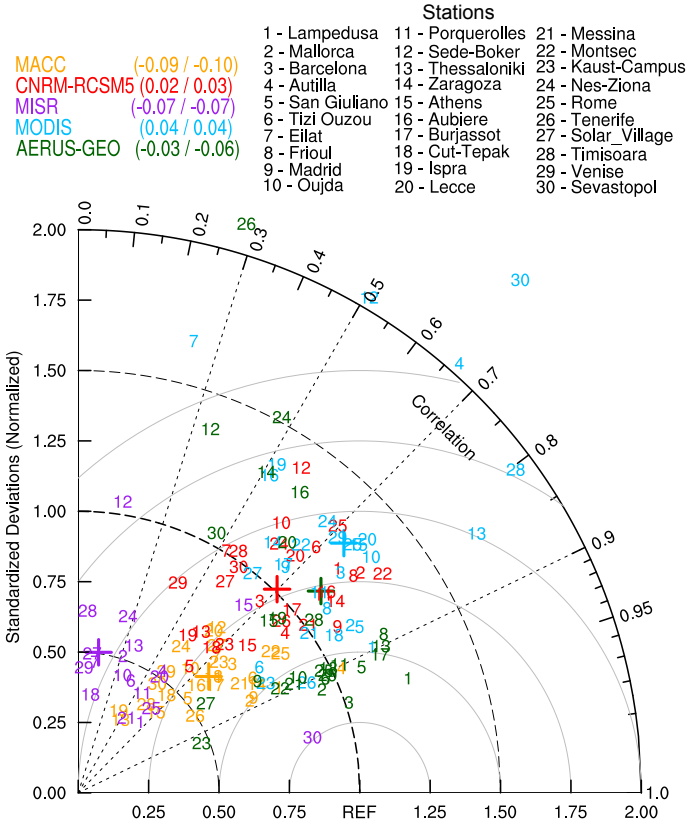

Fig. 4. Taylor diagram evaluating CNRM-RCSM5 (red), MACC (orange) and satellite (MODIS, blue and AERUS-GEO, green) data against 30 AERONET ground-based observations in terms of daily AOD in summer 2012. Averages over the 30 stations for each dataset are indicated with crosses. The mean bias against AERONET is indicated in the caption between brackets (all the 30 stations / the 9 stations located to the north of 33°N).

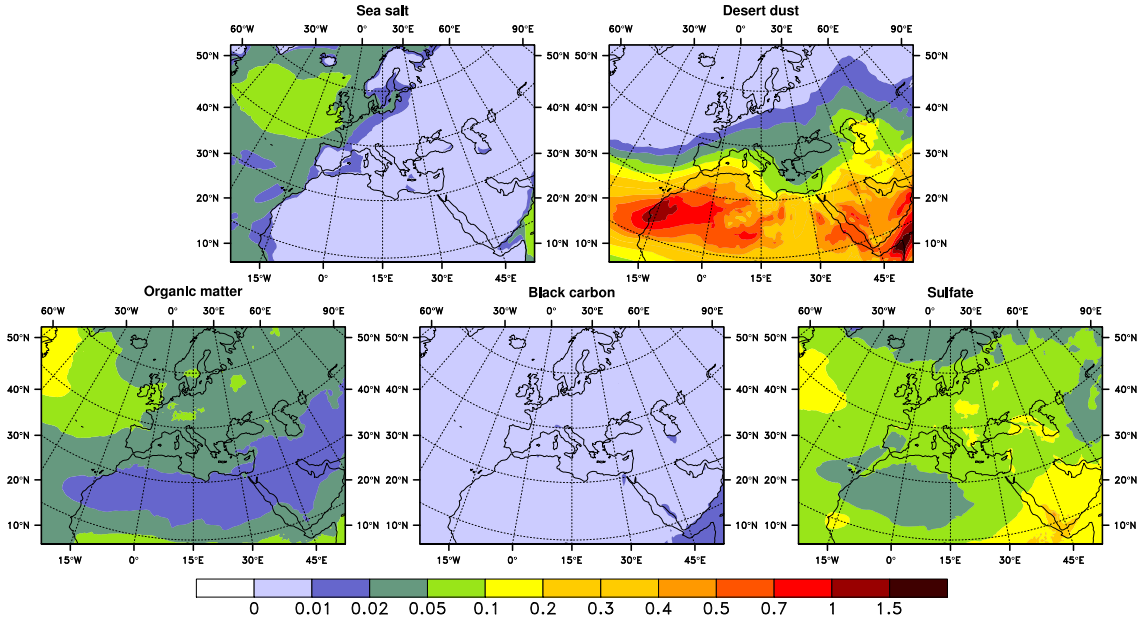

Fig. 5. Mean aerosol optical depth at 550 nm in summer 2012 (JJA) simulated by CNRM-RCSM5 for the five aerosol types (sea-salt, desert dust, organic matter, black carbon and sulphate).

Europe	CNRM-RCSM5	MACC	NAB13	MODIS	MISR	AERUS-GEO
Sea-salt	0.01	0.02	0.00 [0.00 - 0.00]	-	-	-
Desert dust	0.04	0.06	0.05 [0.04 - 0.05]	-	-	-
Organic matter	0.04	0.02	0.02 [0.02 - 0.03]	-	-	-
Black carbon	0.01	0.01	0.01 [0.01 - 0.01]	-	-	-
Sulphate	0.08	0.10	0.10 [0.08 - 0.12]	-	-	-
Total	0.18	0.21	0.18 [0.16 - 0.20]	0.16	0.15	0.15
Mediterranean						
Sea-salt	0.01	0.02	0.01 [0.00 - 0.01]	-	-	-
Desert dust	0.11	0.10	0.12 [0.10 - 0.13]	-	-	-
Organic matter	0.03	0.02	0.01 [0.01 - 0.02]	-	-	-
Black carbon	0.01	0.01	0.01 [0.00 - 0.01]	-	-	-
Sulphate	0.07	0.09	0.08 [0.07 - 0.10]	-	-	-
Total	0.23	0.24	0.23 [0.19 - 0.25]	0.20	0.22	0.18
Africa						
Sea-salt	0.00	0.01	0.00 [0.00 - 0.00]	-	-	-
Desert dust	0.37	0.18	0.31 [0.25 - 0.33]	-	-	-
Organic matter	0.02	0.02	0.01 [0.01 - 0.02]	-	-	-
Black carbon	0.01	0.01	0.01 [0.01 - 0.01]	-	-	-
Sulphate	0.05	0.07	0.08 [0.06 - 0.09]	-	-	-
Total	0.45	0.29	0.41 [0.33 - 0.44]	0.33	0.32	0.21

Table 3. Total AOD and components for the five aerosol types simulated by CNRM-RCSM5 and the MACC reanalysis in summer 2012 over Europe (continental area up to 30°E), the Mediterranean Sea and northern Africa (continental area up to 25°N). Averages in summer from NAB13, the climatology of Nabat et al. (2013), have also been indicated with the minimum and maximum summer values (period 2003-2009). Total AOD from satellite data (MODIS, MISR, AERUS-GEO) is also given.

median. Over the Mediterranean Sea, a good agreement is shown between CNRM-RCSM5 (0.23 for total AOD), MACC (0.24) and NAB13 (0.23). In addition, the proportion between the different aerosol types is similar in the three datasets. However, as in Europe, satellite data have lower AOD (between 0.18 and 0.22).

More variability is noted with regards to AOD over northern Africa, notably because of the dust component. CNRM-RCSM5 shows higher AOD (0.45) than NAB13 (0.41), MACC (0.32) and the satellite data (between 0.21 and 0.33). However, interannual variability is stronger in this region as shown by the larger amplitude in NAB13 (0.33 - 0.44). Moreover, MACC does not assimilate AOD over the Sahara because the standard algorithm of MODIS cannot retrieve AOD on bright surface, so that an underestimation of dust aerosols in MACC had been identified (Nabat et al., 2013).

In summary, the evaluation of AOD for each aerosol type is complicated because of the heterogeneity between the different datasets, but the contribution of aerosol types to AOD in CNRM-RCSM5 is close to the one in MACC and NAB13. It is worth mentioning that CNRM-RCSM5 does not include the nitrate component. However, dust aerosols constitute the main focus of the following paragraphs.

3.4 Dust extinction vertical profile

CNRM-RCSM5 has shown its ability to reproduce correctly AOD daily evolution, which is a parameter often evaluated

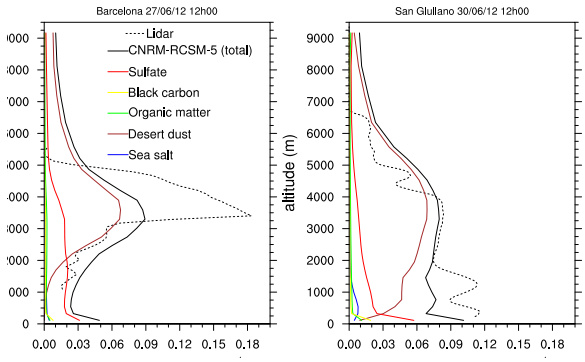

Fig. 6. Aerosol extinction coefficient simulated by CNRM-RCSM5 (full black lines) and observed by a ground-based lidar (dotted black lines) in Barcelona on 27th June at 12UTC (left) and in San Giuliano (Corsica) on 30th June 2012 at 12UTC (right). The different colored lines represent the contribution of each aerosol type to the extinction coefficient.

in climate models. However, aerosol direct and semi-direct forcing also depends on the profile and size distribution of particles, rarely evaluated given the scarcity of observations, and affected by large uncertainties (Textor et al., 2006). Even if total AOD is necessary to evaluate AOD against in-situ or satellite measurements that cannot separate the different aerosol types, more attention is now given to the dust component which is the focus of the study. The TRAQA campaign

has well documented a dust outbreak over the Mediterranean Sea, which is useful for this evaluation. However a deeper evaluation of the other aerosol components is out of the scope of the paper.

The dust plume observed in the TRAQA campaign comes from the uplift of dust particles in western Africa between 21st and 23rd June. These particles have been transported along the African coast up to southern Spain, driven by the presence of a low pressure system over Morocco and a high pressure area over the Azores. From 26th June, a low formed in the bay of Biscay generated a southwesterly flow bringing the dust plume over northern Spain. Successively moving to the southeast, dust particles have also been transported over the Mediterranean Sea. Figure 6 presents the vertical distribution of aerosols during the dust outbreak observed by lidars in the TRAQA campaign in terms of extinction coefficient in Barcelona at 532 nm and in San Giuliano at 355 nm. Dust aerosols first reach Spain on 27th June, transported in the mid-troposphere, as noted in the profile between 2000 and 5000 m with a maximum extinction (0.18 km^{-1}) at 3500 m. The two-component elastic lidar inversion algorithm constrained with an AERONET AOD of 0.32 gave a column-equivalent lidar ratio of 54 sr. This value is in the range of 50 – 70 sr established by Tesche et al. (2009) of desert dust lidar ratio observations by Raman lidar, which makes us confident with the result of the lidar inversion. The altitude of these dust particles is similar in CNRM-RCSM5, despite an underestimation of the intensity of the dust outbreak and a slight overestimation in the higher layers. Under this dust layer, the presence of sulphate aerosols is noted in the model, with an extinction coefficient close to observations (0.03 km^{-1}). In San Giuliano, where the dust plume has arrived three days later, its altitude is also similar in CNRM-RCSM5 and observations: between 2000 and 5000m. As in Barcelona, extinction is slightly overestimated in the high troposphere (above 6500m).

In summary, the comparison between these lidar profiles and the dust extinction simulated profiles has shown that CNRM-RCSM5 was able to simulate the different altitudes of dust aerosols, even if it should be mentioned that two profiles are not sufficient to conclude. This kind of comparison would need to be done for other places and situations, but it is a difficult exercise as evaluating only the aerosol vertical distribution implies to find cases where adequate observations are available and where the model correctly simulates the transport of dust aerosols.

3.5 Dust vertical size distribution

Size distribution is also an essential physical parameter for aerosol-climate studies, as optical properties depend on the particle size. Figure 7 presents the size distribution observed during a sounding realized by the ATR42 during the TRAQA campaign, as well as the simulated distribution. Note that the bin scheme used in CNRM-RCSM5 does not enable the model to reproduce exactly the observed distribution, but the division in 3 bins for dust particles notably can still be evaluated. This sounding took place in the Mediterranean Sea (43.05°N, 9.55°E) on 29th June, when the dust plume has been transported over this area. In the lower layers, a first maximum is observed in the smallest particles (around 0.1 μm), probably due to sulphate aerosols, as represented by CNRM-RCSM5. The observed distribution shows that mass concentration is higher for larger particles, especially between 2000 and 4000m, where dust aerosols are located. This distribution is simulated by CNRM-RCSM5, notably between 2000 and 3000m. Above 3000m, coarse particles (larger than 2.0 μm) are underestimated. However, these particles have less impact on extinction in SW radiation than submicronic particles, but they could play a role in other processes (e.g. deposition).

These results finally show that the aerosol vertical and size distributions simulated by CNRM-RCSM5 reproduce the main patterns seen in observations from the TRAQA campaign, even if the simulated profile in Barcelona shows an underestimated extinction peak between 3 and 5 km in altitude.

To summarize, ~~CNRM-RCSM has shown its ability~~ to simulate the evolution of aerosols during summer 2012 in terms of spatial pattern and daily variability, as well as the vertical profiles and size distribution of dust particles. This model will be used in the following section, to study the impact of dust outbreaks on meteorological parameters (radiation, temperature) in summer 2012. In addition, an intercomparison modeling study about this dust event observed in the TRAQA campaign will be the subject of a parallel study led by Sara Basart.

4 Aerosol radiative effects

As seen previously in the AOD temporal series, the Mediterranean basin has been affected by frequent dust outbreaks in summer 2012. This section aims at assessing their impact on different meteorological parameters.

4.1 Direct radiative forcing

Figure 8 first shows the daily direct SW radiative forcing (DRF) of aerosols in PROG. DRF is calculated on-line during the simulation, calling twice the radiation code: with and without aerosols. A negative forcing of aerosols at the surface is noted. It is stronger over regions under dust influence: northern Africa, Arabian peninsula and the tropical Atlantic ocean, reaching -20 to -50 Wm^{-2}, in line with Nabat et al. (2014). Over Europe and northern Atlantic, aerosol DRF ranges from -10 to -15 Wm^{-2}, notably because of sulphate aerosols. Compared to estimations from literature such as the studies of di Sarra et al. (2008) and Di Biagio et al. (2010) who have respectively found an average DRF of -30 and -26

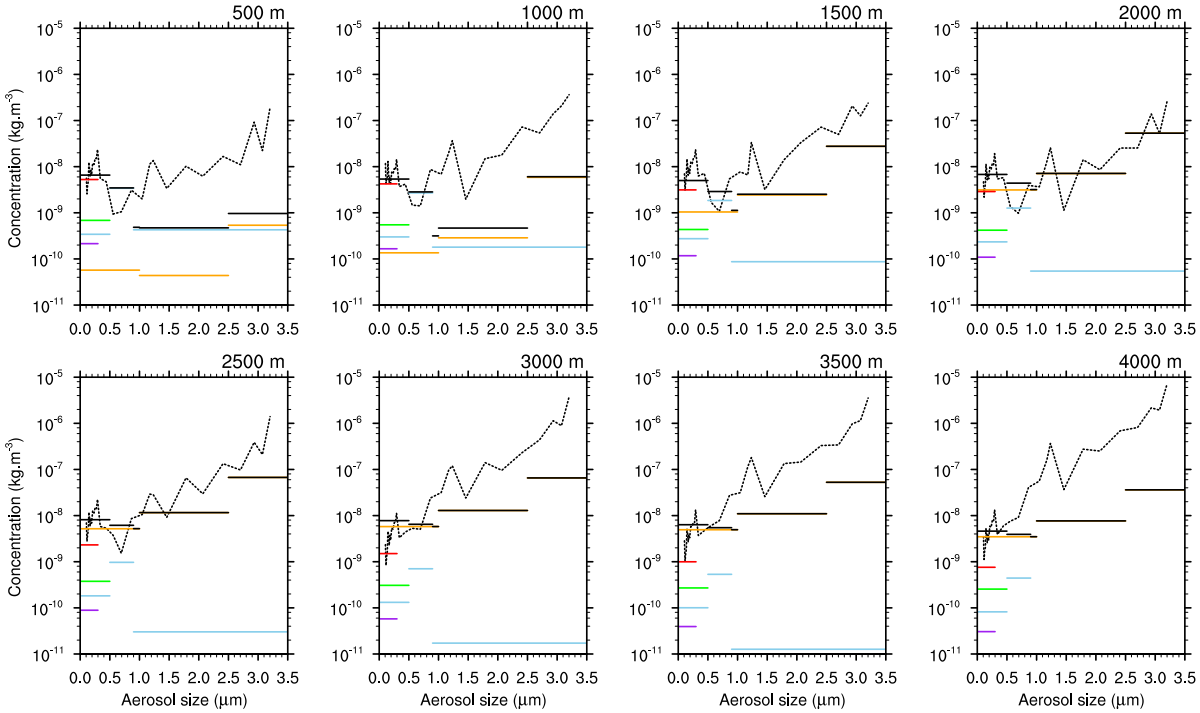

Fig. 7. Dust particle size distribution observed by the PCASP instrument onboard ATR42 (flight 22) on 29th June at 8UTC (dashed black lines), the dust refractive index has been adjusted (1.53 - 0.002i). Full colored lines indicate the aerosol concentration for each aerosol bin of CNRM-RCSM5 (red = sulphate, blue = sea salt, orange = dust, green = organic matter and purple = black carbon), while full black lines indicate the total concentration (kg.m^{-3}).

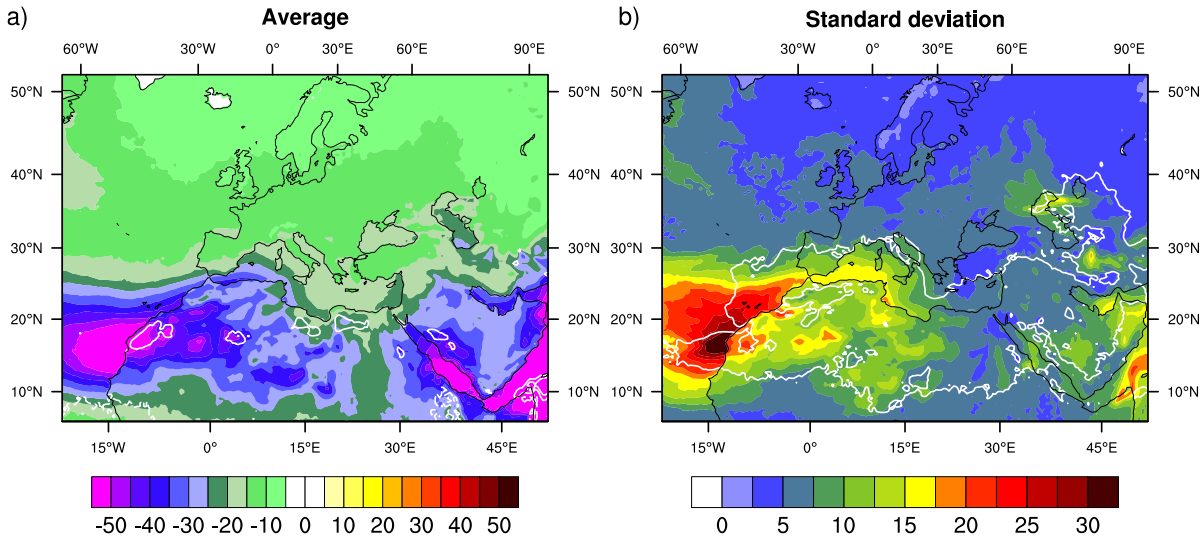

Fig. 8. Aerosol SW direct radiative forcing (DRF): a) Average in summer 2012 for PROG (colors) and the PROG-PROG-M difference (white lines, interval is 5 Wm^{-2}). b) Standard deviation of daily DRF for PROG (colors). The white line indicated the region where the ratio between the standard deviations of PROG and PROG-M is higher than 2.

Wm^{-2} in Lampedusa, the values given by CNRM-RCSM5 have the same order of magnitude, even if they can reach larger forcings. Also note that the Atlantic Ocean off Africa, under the influence of dust export, shows the highest variability.

4.2 At the daily scale

As dust aerosols can interact with solar and thermal radiation, consequences on meteorological parameters such as surface radiation and temperature might be expected. In the present work, an effort has been made to gather colocalized measurements of AOD, SW radiation and 2-meter temperature or sea surface temperature. The list of the 14 corresponding stations in the Mediterranean basin used in this study is presented in Table 1.

Daily series of solar surface radiation (SSR), cloud cover and surface temperature are presented in details for two stations representative of the Mediterranean basin, namely Lampedusa (LAM) and the buoy in the Gulf of Lions (LIO). Lampedusa is located in an island close to dust-emitting regions where clear-sky conditions are frequent in summer, while LIO is in the northwestern Mediterranean, where more clouds are observed. Figures 9 and 10 present respectively in LAM and in LIO the daily series of AOD, downward SSR, cloud cover and surface temperature (resp. 2m-temeprature and SST), observed and simulated by PROG, PROG-M and NO.

First of all, NO is the only CNRM-RCSM5 simulation to have a high bias against observed SSR (+18.0 Wm^{-2} in LAM, 31.2 Wm^{-2} in LIO), compared to PROG-M (-6.0 Wm^{-2} in LAM, 13.6 Wm^{-2} in LIO) and PROG (-3.5 Wm^{-2}, 15.9 Wm^{-2} in LIO), due to the absence of aerosols in NO. While the aerosol climatology is enough to reduce the bias in PROG-M, PROG has the highest temporal correlation (0.87 against 0.81 for NO and 0.85 for PROG-M in LAM), and its standard deviation is the closest to observations (a ratio of 0.88 against 0.74 both for NO and PROG-M in LAM). Indeed, PROG-M and NO clearly miss some variations of SSR. When AOD is high (e.g. 21/06, 3-12/07, 29/07, 7/08 in LAM, 19/06, 27/07, 20/08 in LIO), PROG-M and NO overestimate SSR, especially in case of low cloud cover. Inversely when AOD is low (e.g. 24/06, 20/07, 10/08 in LAM, 5/06, 27/08 in LIO), PROG-M underestimates SSR while NO benefits in this case from the absence of aerosols. ERA-Interim, which has a monthly aerosol climatology as in PROG-M, except that the aerosol climatology used in ERA-Interim (Tegen et al., 1997) is probably less realistic, also simulates radiation variations lower than observed. As a result, the effect of aerosols on surface radiation has been identified in both stations.

With regards to land surface temperature in LAM and SST in LIO, while PROG-M and PROG are on average cooler than NO because of the aerosol forcing, the three CNRM-RCSM5 simulations have similar temporal correlations (between 0.72 and 0.73 for LAM, 0.98 for SST in LIO). Even during dust outbreaks, it is not possible to state that average temperature in PROG is closer to observations. With regards to standard deviations, the daily variability is reduced in PROG (0.89 in LAM against 0.92 for PROG-M and 0.95 for NO). The aerosol forcing during dust events could indeed decrease the maximum daily temperature, while the effect of dust particles on thermal surface radiation (TSR) could increase night-time temperature, and thus reduce T2m diurnal variability.

In order to confirm these results in the other stations, the evaluation of surface radiation and 2m-temperature for the three simulations and the ERA-Interim reanalysis in the 14 stations is presented respectively in Tables 4 and 5. As far as radiation is concerned, the bias is reduced both in PROG and PROG-M, reaching a level close to ERA-Interim (between 11 and 13 Wm^{-2}). A net improvement is noted in temporal correlation, since it is higher in PROG than in PROG-M and NO in every station. Daily variability in SSR is also higher in PROG for most stations, representing an improvement compared to observations except where this variability was already overestimated (e.g. Ajaccio). It is worth mentioning that in Sede-Boker PROG is getting closer to observations by reducing SSR variability. A misrepresentation of cloud processes could also explain some of the discrepancies with observations. The lack of cloud cover in CNRM-RCSM shown in Nabat et al. (2014) could explain the remaining bias. ERA-Interim that does not have the daily aerosol variations and consequently misses some peaks in surface radiation, succeeds in getting a high average correlation coefficient (0.79) probably because of a better representation of clouds. Moreover, changes in water vapour column amount may also affect the SSR to a lesser extent.

As far as surface temperature is concerned, no change in correlation coefficient is noted. The PROG simulation is cooler than NO and PROG-M, increasing the negative bias. Nevertheless the daily variability is slightly reduced, getting closer to observed variability. In addition, it is worth mentioning ERA-Interim has the highest scores in terms of correlation and variability (standard deviation), probably benefiting from the assimilation of surface temperature (Dee et al., 2011).

As a result, these comparisons show that the prognostic aerosol scheme used in PROG enables the model to better reproduce the evolution of surface radiation, that cannot be done properly with an aerosol climatology. However no improvement has been shown in the scores of land and sea surface temperature. However, aerosol maxima over the Mediterranean could be associated to particular weather conditions which are responsible for effects on radiation and temperature that are not due to aerosols. That is the reason why a composite study to isolate the effect of dust aerosols is carried out in the following section.

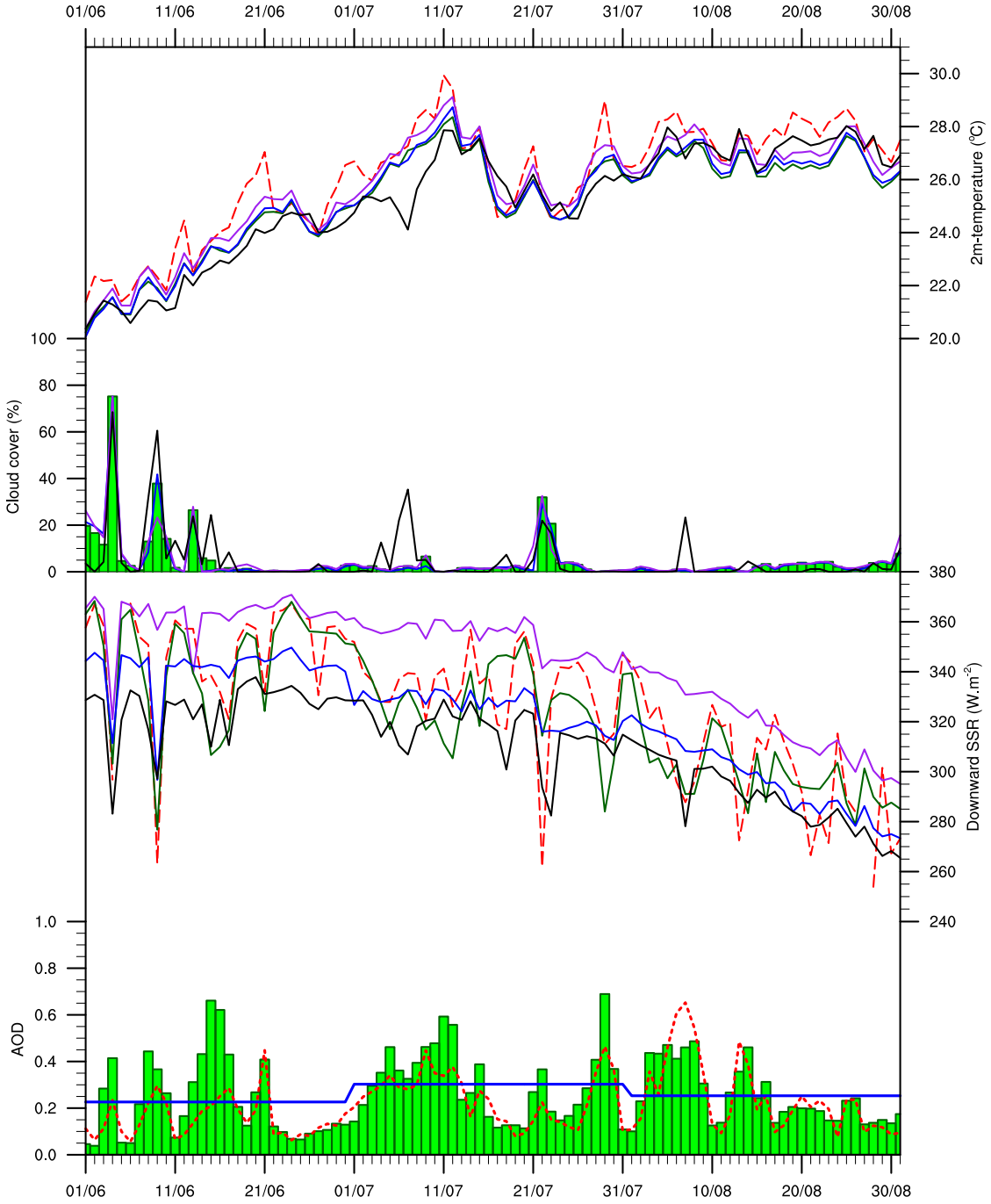

Fig. 9. 2m-temperature (°C, curves), cloud cover (%, green bars for PROG, curves for the other simulations), downward SSR (Wm^{-2}, curves) and AOD (green bars for PROG, blue line for PROG-M), from top to bottom, in Lampedusa (Italy) for PROG (green), PROG-M (blue), NO (purple), ERA-Interim (black) and observations (dashed red).

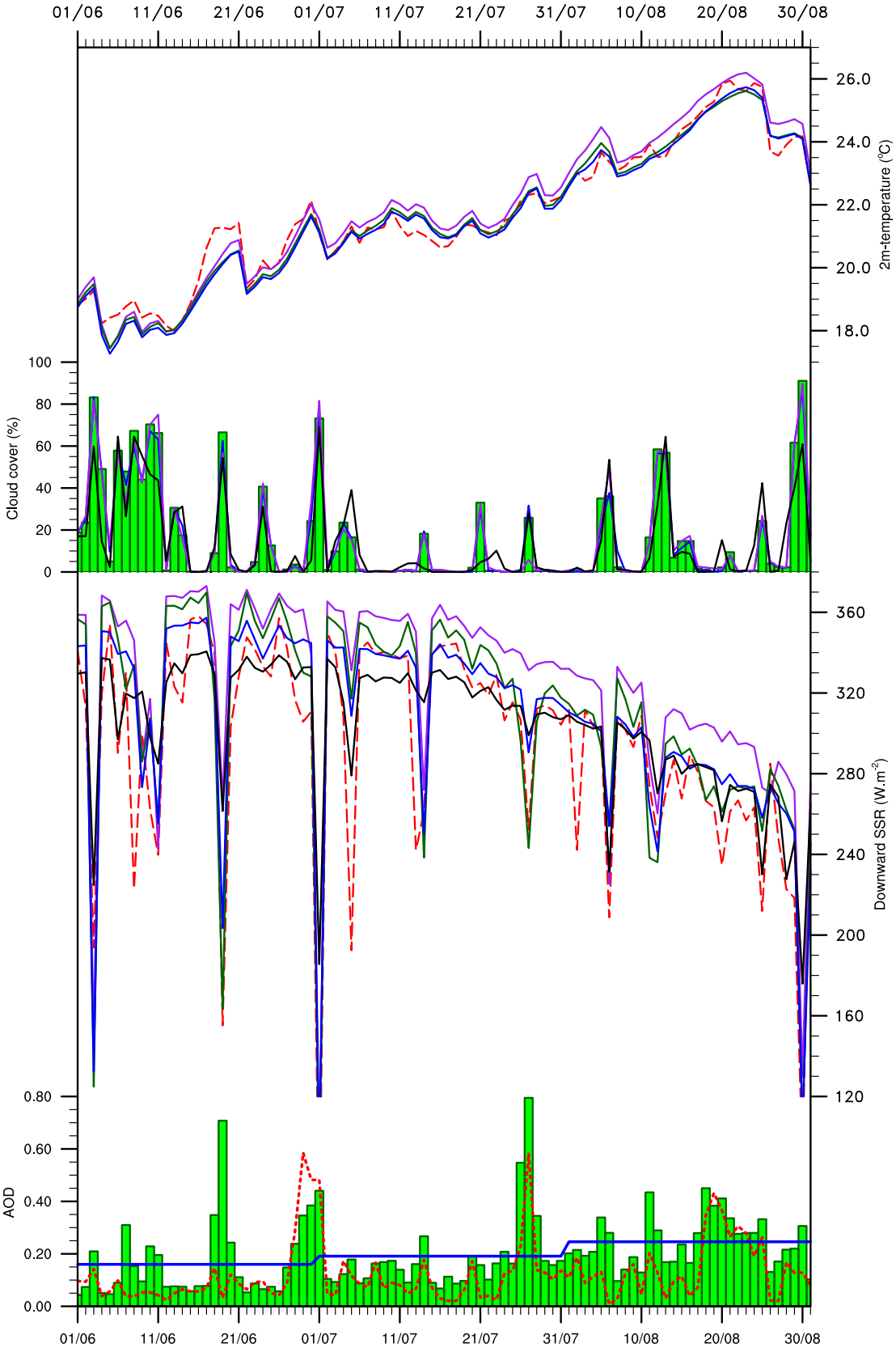

Fig. 10. Same as Figure 9 but for the buoy in the Gulf of Lions (LIO).

Bias	MUR	BAR	MAL	ALI	AJA	CAR	MON	NIC	PER	FES	LIO	AZU	LAM	SED	MOY
NO	31.0	2.8	54.3	39.0	18.0	22.3	35.9	37.6	34.7	48.2	31.2	35.1	18.0	5.6	29.6
PROG-M	7.6	-8.5	35.1	18.1	2.4	10.1	20.8	19.6	19.3	13.6	13.6	16.6	-6.0	-13.4	10.6
PROG	9.7	-7.5	36.0	21.2	5.1	11.5	24.0	22.9	21.0	16.5	15.9	19.1	-3.5	-11.7	12.9
ERA-Interim	12.8	4.6	53.7	25.4	-1.0	-4.3	17.0	10.1	27.7	34.7	10.2	7.2	-16.8	-12.9	12.0
Corr.															
NO	0.72	0.76	0.66	0.62	0.87	0.89	0.71	0.67	0.76	0.39	0.87	0.86	0.81	0.84	0.75
PROG-M	0.76	0.77	0.65	0.67	0.89	0.87	0.70	0.69	0.77	0.49	0.88	0.87	0.85	0.89	0.76
PROG	0.77	0.79	0.69	0.74	0.89	0.91	0.75	0.69	0.78	0.53	0.89	0.90	0.87	0.90	0.79
ERA-Interim	0.79	0.81	0.88	0.81	0.88	0.88	0.77	0.68	0.75	0.37	0.90	0.76	0.87	0.88	0.79
St. Dev.															
NO	0.79	1.20	0.84	1.16	1.11	0.96	0.97	0.81	0.96	0.93	0.92	1.00	0.74	1.15	0.97
PROG-M	0.79	1.10	0.82	1.11	1.10	0.86	0.92	0.81	0.93	0.94	0.91	1.04	0.74	0.99	0.93
PROG	0.95	1.16	1.01	1.20	1.17	0.94	0.98	0.88	0.99	1.01	1.01	1.12	0.88	1.07	1.03
ERA-Interim	0.58	0.72	0.69	0.78	0.78	0.77	0.69	0.72	0.63	0.53	0.61	0.90	0.67	0.92	0.71

Table 4. Evaluation of daily SSR simulated by NO, PROG-M, PROG and ERA-Interim against 14 ground-based measurements located around the Mediterranean basin, in terms of bias (Wm^{-2}), temporal correlation coefficient and standard deviation ratio.

Bias	MUR	BAR	MAL	ALI	AJA	CAR	MON	NIC	PER	FES	LIO	AZU	LAM	MOY
NO	-0.3	-1.6	1.2	-0.5	-1.5	0.9	-1.5	-0.0	-2.0	0.0	0.6	1.6	-0.4	-0.3
PROG-M	-0.6	-1.7	0.8	-0.7	-1.7	0.8	-1.7	-0.3	-2.2	-0.4	0.4	1.4	-0.8	-0.5
PROG	-0.8	-1.9	0.7	-0.8	-1.8	0.8	-1.7	-0.3	-2.2	-0.4	0.4	1.4	-0.8	-0.6
ERA-Interim	-2.7	-2.8	-1.2	-0.1	0.1	-2.8	-1.3	-1.4	-1.6	-0.9	0.4	0.6	-0.5	-1.1
Corr.														
NO	0.76	0.87	0.91	0.76	0.88	0.92	0.77	0.79	0.87	0.91	0.97	0.82	0.96	0.86
PROG-M	0.77	0.89	0.92	0.77	0.88	0.92	0.77	0.81	0.88	0.92	0.97	0.81	0.96	0.86
PROG	0.76	0.88	0.92	0.75	0.88	0.92	0.77	0.80	0.89	0.92	0.97	0.81	0.96	0.86
ERA-Interim	0.88	0.98	0.88	0.75	0.86	0.92	0.89	0.90	0.89	0.96	0.93	0.81	0.90	0.89
St. Dev.														
NO	1.36	1.09	1.25	1.44	1.45	1.16	0.90	1.42	1.37	0.96	1.14	1.08	0.97	1.20
PROG-M	1.31	1.10	1.26	1.38	1.45	1.15	0.87	1.41	1.37	0.96	1.10	1.05	0.95	1.18
PROG	1.27	1.04	1.20	1.34	1.42	1.12	0.87	1.36	1.35	0.97	1.08	1.03	0.93	1.15
ERA-Interim	1.04	0.76	0.92	1.36	1.05	1.03	0.93	0.98	0.82	0.88	0.95	0.99	1.00	0.98

Table 5. Evaluation of daily 2m-temperature simulated by NO, PROG-M, PROG and ERA-Interim against 13 ground-based measurements located around the Mediterranean basin, in terms of bias (°C), temporal correlation coefficient and standard deviation ratio.

4.3 Composite analysis

4.3.1 Methodology

This section aims at highlighting the simulated and observed differences between days of high aerosol load and the set of all the days in terms of several meteorological parameters (radiation, temperature, cloud cover, ...). For the fourteen stations defined previously, the days of high AOD, called thereafter "dusty" days as dust aerosols are mostly responsible for these AOD maxima, have been selected over the 92 days of the summer 2012 (June-July-August). A day is considered as a dusty day provided that observed AOD is higher than 0.2 and that simulated dust AOD in PROG is higher than 0.2. Days when observations were not available have been removed.

Average differences for several parameters have then been calculated between the dusty days and the set of all the days, for the three simulations (NO, PROG-M and PROG) and observations. The differences obtained for NO will enable us to estimate the meteorological effect, only due to changes in weather parameters (cloud cover, wind, etc.) without considering the aerosols, for PROG-M the average effect of having an aerosol climatology, and for PROG the added value of prognostic aerosols. The objective is to isolate the effects of aerosols from weather changes that are systematically observed during dust outbreaks. This method is first presented for the station of Murcia, whose results are representative of the whole Mediterranean basin, and then generalized to the fourteen stations.

4.3.2 Case of Murcia

In Murcia, 23 days have been identified as dusty days over the 83 days when observations are available, results are presented in Table 6. First of all, the difference in AOD between dusty days and the set of all the days is similar in the observations and PROG, confirming the ability of CNRM-RCSM5 to reproduce aerosol daily variability, and making it possible the comparison for other parameters. In PROG-M, the slight difference (-0.01) is due to the fact that the number of dusty days varies from one month to another (AOD is monthly constant in PROG-M); no difference in NO since no aerosols are simulated. The higher AOD during dusty days leads to a decrease in downward SSR. The difference with the set of all the days reaches -22 Wm^{-2} against only -6 and -7 Wm^{-2} for respectively NO and PROG-M, while measurements in the station show a difference of -19 Wm^{-2}. The difference in NO (-6 Wm^{-2}) can be considered as the "weather effect", that is due to the choice of the days (meteorological and astronomical variations). The duration of sunshine indeed varies during summer, and reaches its maximum at the solstice (21 June), which can explain a part of the radiation differences in NO, in addition to changes in cloud cover. PROG-M, which has a monthly climatology of aerosols, is useful to identify changes in atmospheric circulation and cloud cover due to a monthly climatology of aerosols (-1 Wm^{-2}). The difference between PROG-M and PROG gives the contribution of the daily variability of aerosols, that is necessary to reproduce observed radiation measurements. Few changes are observed in cloud cover and TSR.

Temperature is also affected by weather changes, as dusty days are 1.6°C higher in NO than the set of all the days. This is probably explained by the predominance of stronger southern fluxes during dusty days that can transport aerosols from Sahara to the Mediterranean basin. Figure 11 indeed shows the average circulation at 850 hPa during dusty days and the set of all the days, indicating a reinforcement of southwesterly winds in southern Spain advecting warm air. However, this increase in temperature during dusty days is lower in PROG than in PROG-M and NO, which is closer to observed variations of temperature. This decrease of -0.2°C is caused by dust aerosols that have reduced incoming solar radiation. A similar impact is observed in soil temperature.

As a result, radiation and temperature in Murcia have been shown to be better reproduced in the PROG simulation, showing the added value of a prognostic scheme compared to monthly climatologies to reproduce local ~~climatic~~ variations.

4.3.3 Generalization

A similar composite study has been carried out for other stations (defined in Table 1) where daily radiation and temperature data were available. Figure 12 presents the results per station for six parameters (AOD, solar and thermal surface radiation, cloud cover, 2m and soil temperature) for the NO, PROG-M and PROG simulations, as well as for observations when available, while the average composites are given in Table 7.

As in Murcia, the difference in AOD between dusty days and the set of all the days is for every station similar in observations (0.22 on average) and the PROG simulation (0.21). The difference in PROG-M comes only from the number of dusty days varying from one month to another. As a consequence, measurements reveal that downward SSR is on average 23 Wm^{-2} lower during dusty days, which is correctly reproduced by PROG (-23 Wm^{-2}). A part of this decrease (-2 Wm^{-2}) is explained by weather changes as simulated by NO, while added an aerosol climatology does not bring significant differences (-3 Wm^{-2}). Besides, the decrease of SSR in dusty days varies from one station to another (ranging from -2 to -53 Wm^{-2}). The amplitude of the increase in AOD on dusty days and changes in weather conditions explain this variability. For example in Mallorca, an increase of 6% in cloud cover on dusty days amplifies the dimming due to aerosol loads.

With regards to downward TSR, an average increase of 14 Wm^{-2} is simulated by PROG on dusty days, but it is mainly due to weather conditions as NO and PROG-M also show an increase of 12 Wm^{-2}. Dust aerosols would consequently only represent an increase of 2 Wm^{-2}. Few LW observations are unfortunately available. The measurements in the Gulf of Lions and in Lampedusa show a lower increase than the simulations.

More observations are available for T2m, revealing a general increase of temperature on dusty days (on average 1.4°C). As in Murcia, this increase is probably due to warm advection caused by southerly to southwesterly winds responsible of these dust outbreaks. NO indeed simulates an average increase of 1.7°C, but reduced to 1.5°C in PROG, indicating the cooling due to dust aerosols, which makes the simulation closer to observations. This improvement is noted in 10 out of the 13 stations considered in the study (Figure 12), these 10 stations being the 9 continental stations and the buoy Azur. The other stations either do not show a cooling (Ajaccio) or this cooling is not in line with observations (buoy of the Gulf of Lions, Lampedusa). For these two latter stations, sea surface temperature also increases on dusty days (up to 2.0°C in the Gulf of Lions in NO), while PROG-M and PROG both alleviate this increase by 0.1°C. However, this reduction cannot be confirmed by observations. Maybe the three-month period is not long enough to identify the daily effects of aerosols on SST. With regards to land soil temperature, a cooling of -0.3°C due to dust aerosols is simulated by PROG, in relationship with the cooling in T2m.

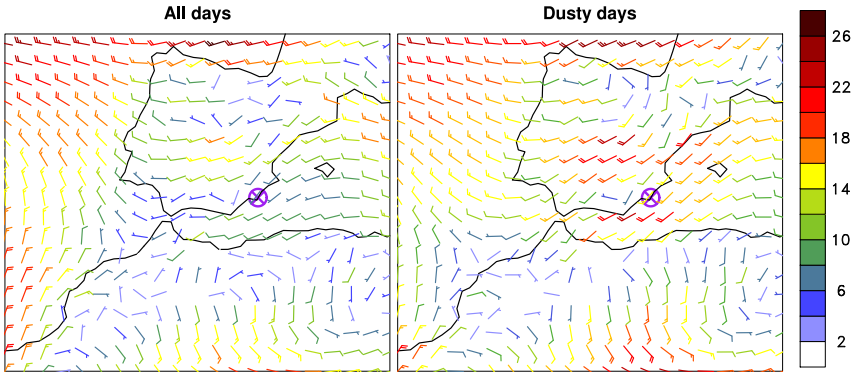

Fig. 11. Average wind (km/h, colored barbs) and geopotential (mgp, black lines) at 850 hPa for the set of all the days (left) and the dusty days (right) defined in Murcia (purple cross).

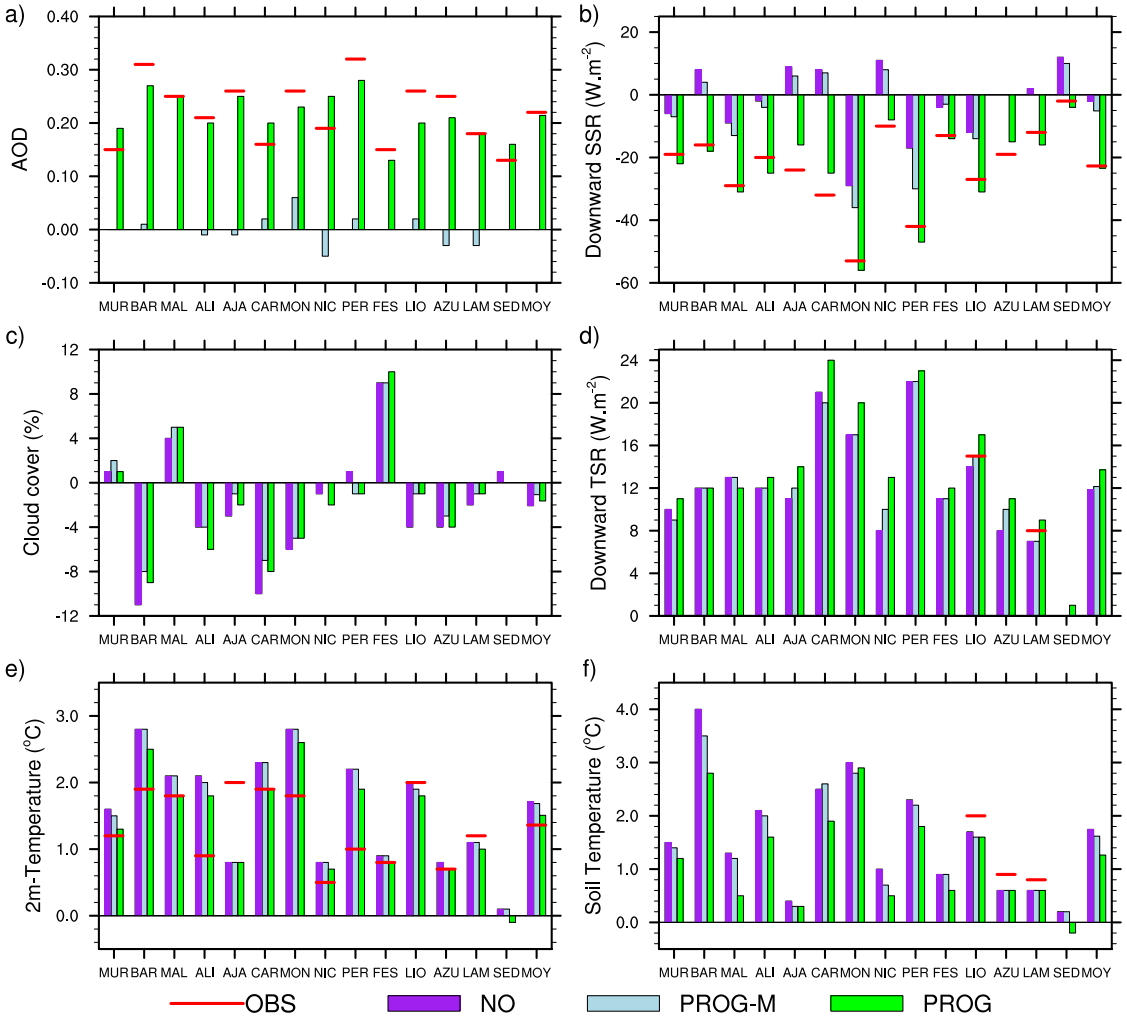

Fig. 12. Average AOD (a), downward SSR (b), cloud cover (c), downward TSR (d), 2m-temperature (e) and soil temperature (f) difference between the dusty and the set of all the days in fourteen stations (presented in Table 1) in summer 2012 for the NO, PROG-M and PROG simulations, as well as observations (AERUS-GEO for AOD, ground-based measurements for the other parameters). For Lampedusa and the buoys in the Gulf of Lions and Azur, 2m-temperature has been replaced by SST.

Parameter	OBS	NO	PROG-M	PROG	Weather	Aerosol (mean)	Aerosol (var)
AOD	0.15	0.00	-0.01	0.19	0.00	-0.01	0.20
SSR	-19	-6	-7	-22	-6	-1	-15
Cloud cover	-	1	2	1	1	1	-1
TSR	-	10	9	11	10	-1	2
T2m	1.2	1.6	1.5	1.3	1.6	-0.1	-0.2
Ts	-	1.5	1.4	1.2	1.5	-0.1	-0.2

Table 6. Composite study for Murcia: differences between dusty days and the set of all the days in observations (OBS), NO, PROG-M and PROG, for AOD, downward SSR (Wm^{-2}), cloud cover (%), downward TSR (Wm^{-2}), 2m-temperature (°C) and soil temperature (Ts, °C). The contribution of the different effects, namely weather, aerosol (mean), and aerosol (variability), have been added.

Parameter	OBS	NO	PROG-M	PROG	Weather	Aerosol (mean)	Aerosol (var)
AOD	0.22	0.00	0.00	0.21	0.00	0.00	0.21
SSR	-23	-2	-5	-23	-2	-3	-18
Cloud cover	-	-2	-1	-2	-2	1	-1
TSR	-	12	12	14	12	0	2
T2m	1.4	1.7	1.7	1.5	2.0	0.0	-0.2
Land soil temperature	-	1.7	1.6	1.3	1.7	-0.1	-0.3
SST	1.3	0.9	0.9	0.9	1.3	0.0	0.0

Table 7. Same as Table 6 but for the average over the 14 stations defined in Table 1.

4.4 Impact of daily aerosol variability on the summer average

The question that can be deduced from the impact of aerosols shown on surface radiation and temperature during dusty days is to know if using an aerosol prognostic scheme instead of a monthly climatology has also an impact on the summer average.

As far as DRF is concerned, average differences in summer 2012 between PROG and PROG-M are presented in Figure 13 both for SW (a) and LW (b) radiation. The intensity of the average aerosol forcing is slightly lower (3 Wm^{-2}) in PROG-M than in PROG for the SW component, while very few differences are observed for LW radiation. Moreover, the daily standard deviation of SW DRF is higher in PROG than in PROG-M, particularly over northern Africa and the Mediterranean Sea, where it is more than twice higher (Figure 8 b). Indeed, dust emission is not a continuous phenomenon, because it is associated with episodes of strong wind over northern Africa. Consequently dust particles show high variability over the Mediterranean basin that PROG-M cannot take into account contrary to PROG. The only daily variations of DRF in PROG-M are due to cloud cover variations, as the aerosol effect can be partially masked by the presence of clouds.

As a consequence, the aerosol effect on surface temperature is on average slightly different in PROG-M compared to PROG (Figure 13 c). The general cooling, due to the presence of aerosols that scatter and absorb incident solar radiation, preventing it from reaching the surface, is either reinforced (e.g. in the southwestern Mediterranean) or alleviated (e.g. in eastern Europe) when using an aerosol interactive scheme instead of a monthly climatology. A similar difference between PROG and PROG-M is found for SST (Figure 13 d). These changes are probably due to the interactions between aerosols and weather conditions. As seen previously in the composite study, the fact that high dust loads often occur in southern fluxes could modify their impact on weather and climate. Moreover, when using an aerosol climatology, the variability of the atmospheric aerosol content is weaker, and the extreme values of AOD are not represented in the model.

Over the Mediterranean, while frequent AOD peaks are observed in the southwest due to frequent dust outbreaks, the latter less often reach the Gulf of Lions, hence less frequent AOD peaks. The AOD standard deviation in PROG is for example 0.22 for the Strait of Gibraltar and only 0.14 for the Gulf of Lions. In result, there are more days in the Strait of Gibraltar (32) where AOD is much higher (difference higher than 0.1) in PROG than in PROG-M, than in the Gulf of Lions (15), despite common averages. Consequently, the aerosol effect can be more important in the Strait of Gibraltar than in the Gulf of Lions, which must explain a cooler SST in the Strait of Gibraltar. In addition, the days when AOD is high in the Gulf of Lions are often cloudy, which alleviate the effect of aerosols. Indeed, dust outbreaks over the northern basins are more frequent under southerly winds (Gkikas et al., 2012), that also favour humidity advection and cloud cover.

In summary, the choice of using an aerosol prognostic scheme instead of a monthly climatology has not only an impact on daily weather ~~and climate variability~~, but also on the summer average. This second impact has never been shown before over the Mediterranean to our knowledge.

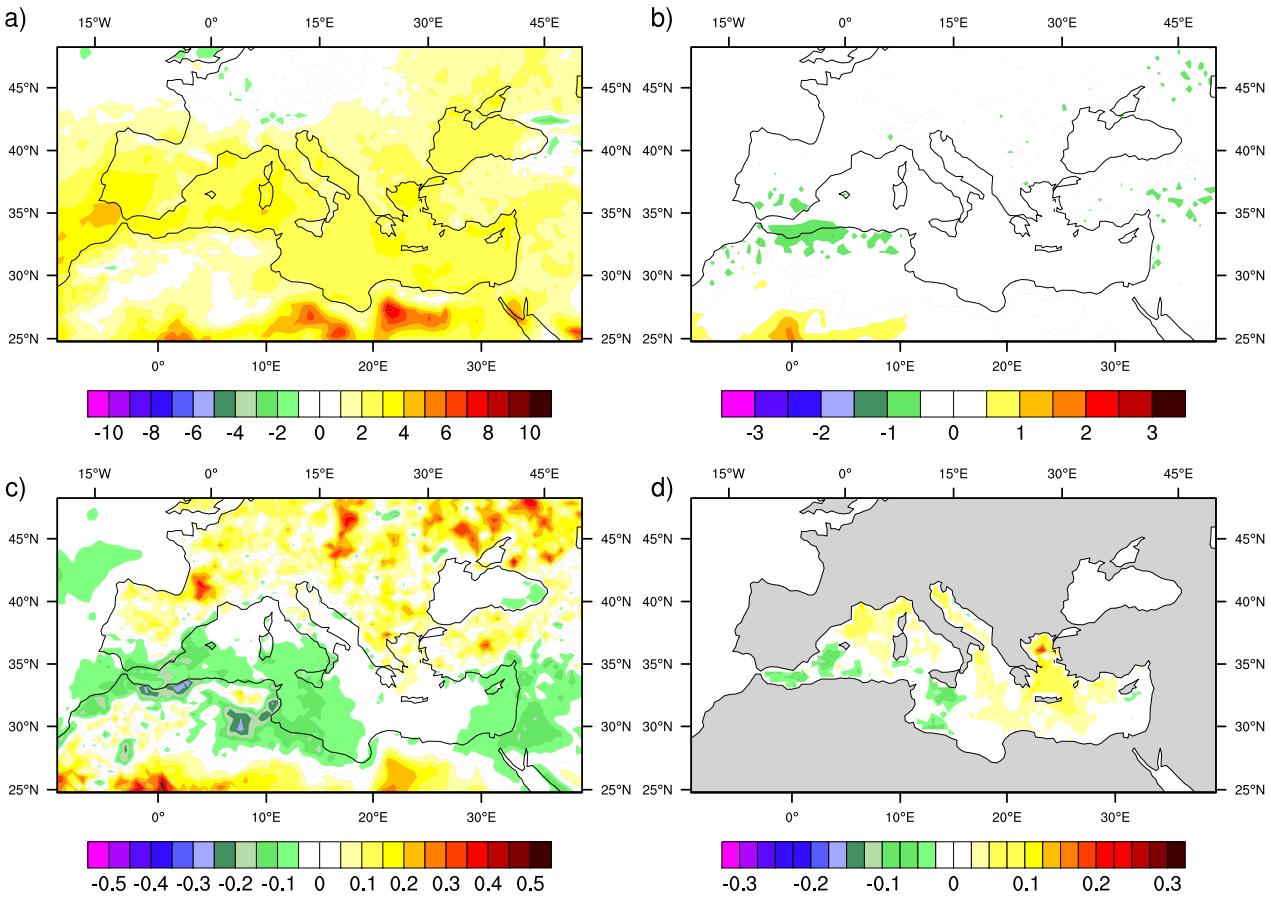

Fig. 13. Average difference in summer 2012 between the PROG and PROG-M simulations in terms of: a) SW surface direct radiative forcing (Wm^{-2}), b) LW surface direct radiative forcing (Wm^{-2}), c) 2m-temperature (°C) and d) sea surface temperature (°C).

4.5 Discussion

This study has shown the radiative ~~and climatic~~ effects of dust aerosols in summer 2012 over the Mediterranean, but some points need to be discussed.

First, the choice to focus on a particular summer has been motivated by the fact that summer 2012 was particularly affected by dust outbreaks. Thus, a high number of dusty days could have been noted, providing an interesting case to estimate the radiative ~~and climatic~~ effects of dust aerosols. However, one can wonder if the results would change during a summer with few dust outbreaks, notably with regards to the impact of the choice of prognostic aerosols. As a matter of fact, the composite study and the analysis of the utility of prognostic aerosols should be redone on a longer period, even if finding adequate observations may represent an obstacle. It would be also interesting to consider the other seasons.

In addition, the choice of using the spectral nudging method may have influenced the results, as it can be seen as a limitation of the effect of aerosols on the atmosphere. Indeed, this relaxation towards the ERA-Interim inside the regional domain could for example prevent aerosols from modifying temperature and humidity profiles above 700 hPa, and thus having stronger semi-direct effects. This point is particularly interesting with regards to the impact of the choice of prognostic aerosols instead of monthly AOD means. Nevertheless, the spectral nudging method is essential to represent the real chronology of dust events, making the comparison to observations possible. With regards to the uncertainties of the model outputs, they will be more deeply evaluated in a multi-model exercise currently carried out in the framework of the TRAQA/ChArMEx campaign.

Finally, the low complexity of the aerosol scheme used in the present work could constitute another limitation. In particular, it does not take into account the detailed processes of the formation of secondary aerosols mainly because of too large numerical cost, nor does it consider the second indirect effect of aerosols because of the huge uncertainties in their parameterizations (Quaas et al., 2009). Moreover, it is essential to keep a low numerical cost in order to be able to carry out easily multi-annual climate simulations with a coupling between the different components of the regional climate system (atmosphere, aerosols, land surface and ocean).

5 Conclusions

A prognostic aerosol scheme has recently been added in the regional climate model ALADIN-Climate, enabling to have for the first time a regional coupled system model (CNRM-RCSM5) including the atmosphere, prognostic aerosols, land surface and the ocean components over the Mediterranean region. Simulations have been carried out in summer 2012 first to evaluate the aerosols produced by the model, and then to estimate the radiative ~~and climatic effects~~ of dust outbreaks over the Mediterranean region.

CNRM-RCSM5 has shown its ability to reproduce the spatial and temporal variability of AOD over the Mediterranean region in summer 2012. The general spatial patterns, notably the locations of regions with high AOD, are in agreement with satellite data, while the distribution in the main different aerosol types is close to the MACC reanalysis and the independent climatology from Nabat et al. (2013). Daily variability is also correctly simulated by the model, since the evaluation against 30 stations from the AERONET network shows a mean bias of 0.02, an average correlation coefficient of 0.70 and an average ratio of standard deviations of 1.01 as good as satellite data. In addition, the TRAQA campaign has provided lidar and airborne measurements of a strong dust outbreak that occurred at the end of June 2012. The aerosol vertical distributions observed in Barcelona and in Corsica show that the model is able to reproduce the altitude of maximum extinction, even if a slight overestimation has been noted in the upper troposphere. With regards to dust size distribution, the 3-bin scheme used in ALADIN-Climate simulates higher mass concentrations for the largest particles, as well as a second maxima for submicronic particles, as observed during the TRAQA campaign.

The simulated aerosol surface SW DRF is negative, ranging from -10 Wm^{-2} in Europe to -50 Wm^{-2} in Africa, in line with previous studies. However, here the aerosol DRF is shown to have much variability when using a prognostic aerosol scheme instead of a monthly climatology. As a consequence, thanks to the prognostic aerosol scheme, downward SSR is better reproduced compared to ground-based measurements from several stations across the Mediterranean, both on days of high AOD (lower SSR) and low AOD (higher SSR), as correlation and standard deviation are improved. The forcing due to the dust outbreaks also causes extra cooling in surface temperature, but insufficient to improve significantly the correlation. However, the average difference between a simulation using a prognostic aerosol scheme and an aerosol climatology show a cooling of 0.1 to 0.2°C both in T2m and SST close to the dust sources, notably in the southwestern Mediterranean. Dynamics can also change in the two simulations, and thus modify surface temperature.

A composite study has been realized in 14 stations across the Mediterranean to identify more precisely the differences between dusty days and the set of all the days. During dusty days, SSR is shown to be reduced on average by 28 Wm^{-2}, mostly because of the dimming of aerosols (-17 Wm^{-2}) but also because of weather conditions (-10 Wm^{-2}). In parallel, dust outbreaks that are responsible of dusty days also bring warm air, which explains that T2m is observed 1.6°C higher on dusty days. This warming is too strong (2.0°C) when considering only an aerosol climatology. The prognostic scheme reduces this average warming of 0.2°C, getting closer to observations.

Finally this study has shown the improvement brought by a prognostic aerosol scheme compared to a monthly climatology in terms of radiation and temperature during a summer. This methodology could be applied on multi-annual simulations to evaluate the impact of prognostic aerosols at the climate scale. Differences could be expected not only in terms of variability but also in average climate as suggested by the differences shown in average SST in summer 2012 in the present work.

Acknowledgements. We would like to thank Meteo-France for the financial support of the first author, and the surface radiation and temperature in French stations. This work is part of the Med-CORDEX initiative (www.medcordex.eu) and a contribution to the HyMeX and ChArMEx programmes. ChArMEx is the atmospheric component of the French multidisplinary program MISTRALS (Mediterranean Integrated Studies aT Regional And Local Scales). ChArMEx-France was principally funded by INSU, ADEME, ANR, CNES, CTC (Corsica region), EU/FEDER, Météo-France, and CEA. The aircraft was operated by SAFIRE. TRAQA was funded by ADEME/PRIMEQUAL and MISTRALS/ChArMEx programmes and Observatoire Midi-Pyrénées. This research has received funding from the French National Research Agency (ANR) projects ADRIMED (contract ANR-11-BS56-0006) and REMEMBER (contract ANR-12-SENV-0001), as well as from the FP7 European Commission project CLIMRUN (contract FP7-ENV-2010-265192). The authors acknowledge AEMET for supplying the data and the HyMeX database teams (ESPRI/IPSL and SEDOO/Observatoire Midi-Pyrénées) for their help in accessing the data. We also thank the PI investigators of the different AERONET stations and their staff for establishing and maintaining all the sites used in the present work. The MACC data comes from the ECMWF website, MACC was funded between 2009 and 2011 as part of the 7th Framework Programme, pilot core GMES Atmospheric Service under contract number 218793. Measurements at Lampedusa were supported by the Italian Ministry for University and Research through Projects NextData and Ritmare. Lidar measurements in Barcelona were supported by the 7th Framework Programme project Aerosols, Clouds, and Trace Gases Research Infrastructure Network (ACTRIS) (grant agreement no. 262254); by the Spanish Ministry of Science and Innovation and FEDER funds under the projects TEC2012-34575, TEC2009-09106/TEC, CGL2011-13580-E/CLI and CGL2011-16124-E/CLI. We also thank Dominique Carrer, Xavier Ceamanos and the ICARE center for the AERUS-GEO dataset. The data of the two Mediterranean buoys were obtained from the HyMeX program, sponsored by grants from MISTRALS/HyMeX and Météo-France

References

Artale, V., Calmanti, S., Carillo, A., Dell'Aquila, A., Herrmann, M., Pisacane, G., Ruti, P. M., Sannino, G., Struglia, M. V., Giorgi, F., Bi, X., Pal, J. S., Rauscher, S., and the PROTHEUS Group: An atmosphere–ocean regional climate model for the Mediterranean area: assessment of a present climate simulation, Climate Dynamics, 35(5), 721–740, doi:10.1007/s00382-009-0691-8, 2010.

Barnaba, F. and Gobbi, G. P.: Aerosol seasonal variability over the Mediterranean region and relative impact of maritime, continental and Saharan dust particles over the basin from MODIS data in the year 2001, Atmospheric, Chemistry and Physics, 4, 2367–2391, 2004.

Benedetti, A., Kaiser, J. W., and Morcrette, J.-J.: [global climate] aerosols [in "state of the climate in 2010"], Bulletin of the American Meteorological Society, 92(6), S65–S67, 2011.

Benkovitz, C. M., Scholz, M. T., Pacyna, J., Tarrason, L., Dignon, J., Voldner, E. C., Spiro, P. A., Logan, J. A., and Graedel, T. E.: Global gridded inventories of anthropogenic emissions of sulfur and nitrogen, Journal of Geophysical Research, 101, 29 239–29 253, 1996.

Bergamo, A., Tafuro, A. M., Kinne, S., Tomasi, F. D., and Perrone, M. R.: Monthly-averaged anthropogenic aerosol direct radiative forcing over the Mediterranean based on AERONET aerosol properties, Atmospheric, Chemistry and Physics, 8, 6995–7014, 2008.

Beuvier, J., Sevault, F., Herrmann, M., Kontoyiannis, H., Ludwig, W., Rixen, M., Stanev, E., Béranger, K., and Somot, S.: Modeling the Mediterranean Sea interannual variability during 1961–2000: Focus on the Eastern Mediterranean Transient, Journal of Geophysical Research, 115, C08 017, doi:10.1029/2009JC005950, 2010.

Carrer, D., Roujean, J.-L., Hautecoeur, O., and Elias, T.: Daily estimates of aerosol optical thickness over land surface based on a directional and temporal analysis of SEVIRI MSG visible observations, Journal of Geophysical Research, 115, D10 208, doi:10.1029/2009JD012272, 2010.

Carrer, D., Ceamanos, X., Six, B., and Roujean, J.-L.: AERUSGEO: a newly available satellite-derived aerosol optical depth product over Europe and Africa, Geophysical Research Letters, p. in press, doi:10.1002/2014GL061707, 2014.

Colin, J., Déqué, M., Radu, R., and Somot, S.: Sensitivity study of heavy precipitation in Limited Area Model climate simulations: influence of the size of the domain and the use of the spectral nudging technique, Tellus, 62A, 591–604, 2010.

Dee, D. P., Uppala, S. M., Simmons, A. J., Berrisford, P., Poli, P., Kobayashi, S., Andrae, U., Balmaseda, M. A., Balsamo, G., Bauer, P., Bechtold, P., Beljaars, A. C. M., van de Berg, L., Bidlot, J., Bormann, N., Delsol, C., Dragani, R., Fuentes, M., Geer, A. J., Haimbergere, L., Healy, S. B., Hersbach, H., Hólm, E. V., Isaksen, L., Kallberg, P., Köhler, M., Matricardi, M., McNally, A. P., Monge-Sanzf, B. M., Morcrette, J.-J., Park, B.-K., Peubey, C., de Rosnaya, P., Tavolato, C., Thépaut, J.-N., and Vitart, F.: The ERA-Interim reanalysis: configuration and performance of the data assimilation system, Quarterly Journal of the Royal Meteorological Society, 137, 553–597, doi:10.1002/qj.828, 2011.

Déqué, M. and Somot, S.: Extreme precipitation and high resolution with Aladin, Idöjaras Quaterly Journal of the Hungarian Meteorological Service, 112(3-4), 179–190, 2008.

Di Biagio, C., di Sarra, A., and Meloni, D.: Large atmospheric shortwave radiative forcing by Mediterranean aerosols derived from simultaneous ground-based and spaceborne observations and dependence on the aerosol type and single scattering albedo, Journal of Geophysical Research, 115, D10 209, doi:10.1029/2009JD012697, 2010.

di Sarra, A., Pace, G., Meloni, D., De Silvestri, L., Piacentino, S., and Monteleone, F.: Surface shortwave radiative forcing of different aerosol types in the central Mediterranean, Geophysical Research Letters, 35, L02 714, doi:10.1029/2007GL032395., 2008.

Gao, X., Pal, J. S., and Giorgi, F.: Projected changes in mean and extreme precipitation over the Mediterranean region from a high resolution double nested RCM simulation, Geophysical Research Letters, 33, L03 706, doi:10.1029/2005GL024954, 2006.

Gibelin, A.-L. and Déqué, M.: Anthropogenic climate change over the Mediterranean region simulated by a global variable resolution model, Climate Dynamics, 20, 327–339, doi:10.1007/s00382-002-0277-1, 2003.

Ginoux, P., Chin, M., Tegen, I., Prospero, J., Holben, B. N., Dubovik, O., and Lin, S.-J.: Sources and distributions of dust aerosols simulated with the GOCART model, Journal of Geophysical Research, 106, 20,255–20,274, 2001.

Giorgi, F. and Lionello, P.: Climate change projections for the Mediterranean region, Global and Planetary Change, 63, 90–104, doi:10.1016/j.gloplacha.2007.09.005, 2008.

Giorgi, F., Coppola, E., Solmon, F., Mariotti, L., Sylla, M. B., Bi, X., Elguindi, N., Diro, G. T., Nair, V., Giuliani, G., Cozzini, S., Guettler, I., O'Brien, T. A., Tawfik, A. B., Shalaby, A., Zakey, A. S., Steiner, A. L., Stordal, F., Sloan, L. C., and Brankovic, C.: RegCM4: model description and preliminary tests over multiple CORDEX domains., Climate Research, 52, 7–29, doi:10.3354/cr01018, 2012.

Gkikas, A., Houssos, E., Hatzianastassiou, N., Papadimas, C., and Bartzokas, A.: Synoptic conditions favouring the occurrence of aerosol episodes over the broader Mediterranean basin, Quarterly Journal of the Royal Meteorological Society, 138, 932–949, doi:10.1002/qj.978, 2012.

Gkikas, A., Hatzianastassiou, N., Mihalopoulos, N., Katsoulis, V., Kazadzis, S., Pey, J., Querol, X., and Torres, O.: The regime of intense desert dust episodes in the Mediterranean based on contemporary satellite observations and ground measurements, Atmospheric Chemistry and Physics, 13, 12 135–12 154, doi:10.5194/acp-13-12135-2013, 2013.

Guelle, W., Schulz, M., Balkanski, Y., and Dentener, F.: Influence of the source formulation on modeling the atmospheric global distribution of the sea salt aerosol, Journal of Geophysical Research, 106, 27,509–27,524, 2001.

Guieu, C., Dulac, F., Desboeufs, K., Wagener, T., Pulido-Villena, E., Grisoni, J.-M., Louis, F., Ridame, C., Blain, S., Brunet, C., Nguyen, E. B., Tran, S., Labiadh, M., and Dominici, J.-M.: Large clean mesocosms and simulated dust deposition: a new methodology to investigate responses of marine oligotrophic ecosystems to atmospheric inputs, Biogeosciences, 7, 2765–2784, doi:10.5194/bg-7-2765-2010, 2010.

Herrmann, M., Somot, S., Calmanti, S., Dubois, C., and Sevault, F.: Representation of spatial and temporal variability of daily wind speed and of intense wind events over the Mediterranean Sea using dynamical downscaling: impact of the regional climate model configuration, Natural Hazards and Earth System Sci-

ences, 11, 1983–2001, doi:10.5194/nhess-11-1983-2011, 2011.

Holben, B. N., Eck, T. F., Slutsker, I., Tanré, D., Buis, J. P., Setzer, A., Vermote, E., Reagan, J. A., Kaufman, Y., Nakajima, T., Lavenu, F., Jankowiak, I., and Smirnov, A.: AERONET-A Federated Instrument Network and Data Archive for Aerosol Characterization, Remote Sensing of Environment, 66, 1–16, doi:10.1016/S0034-4257(98)00031-5, 1998.

Holben, B. N., Tanré, D., Smirnov, A., Eck, T. F., Slutsker, I., Abuhassan, N., Newcomb, W. W., Schafer, J. S., Chatenet, B., Lavenu, F., Kaufman, Y. J., Castle, J. V., Setzer, A., Markham, B., Clark, D., Frouin, R., Halthore, R., Karneli, A., O'Neill, N. T., Pietras, C., Pinker, R. T., Voss, K., and Zibordi, G.: An emerging ground-based aerosol climatology: Aerosol optical depth from AERONET, Journal of Geophysical Research, 106, 12,067–12,097, doi:10.1029/2001JD900014, 2001.

Huneeus, N., Schulz, M., Balkanski, Y., Griesfeller, J., Prospero, J., Kinne, S., Bauer, S., Boucher, O., Chin, M., Dentener, F., Diehl, T., Easter, R., Fillmore, D., Ghan, S., Ginoux, P., Grini, A., Horowitz, L., Koch, D., Krol, M. C., Landing, W., Liu, X., Mahowald, N. M., Miller, R., Morcrette, J.-J., Myhre, G., Penner, J., Perlwitz, J., Stier, P., Takemura, T., and Zender, C. S.: Global dust model intercomparison in AeroCom phase I, Atmospheric, Chemistry and Physics, 11, 7781–7816, doi:10.5194/acp-11-7781-2011, 2011.

Israelevich, P., Ganor, E., Alpert, P., Kishcha, P., and Stupp, A.: Predominant transport paths of Saharan dust over the Mediterranean Sea to Europe, Journal of Geophysical Research, 117, D02 205, doi:10.1029/2011JD016482, 2012.

Jaeglé, L., Quinn, P. K., Bates, T. S., Alexander, B., and Lin, J.-T.: Global distribution of sea salt aerosols: new constraints from in situ and remote sensing observations, Atmospheric Chemistry and Physics, 11, 3137–3157, doi:10.5194/acp-11-3137-2011, 2011.

Kahn, R. A., Gaitley, B. J., Martonchik, J. V., Diner, D. J., Crean, K. A., and Holben, B.: Multiangle imaging spectroradiometer (misr) global aerosol optical depth validation based on 2 years of coincident aerosol robotic network (aeronet) observations, Journal of Geophysical Research, 110, D10S04, doi:10.1029/2004JD004706, 2005.

Kahn, R. A., Gaitley, B. J., Garay, M. J., Diner, D. J., Eck, T. F., Smirnov, A., and Holben, B. N.: Multiangle Imaging SpectroRadiometer global aerosol product assessment by comparison with the Aerosol Robotic Network, Journal of Geophysical Research, 115, D23 209, doi:10.1029/2010JD014601, 2010.

Knippertz, P. and Todd, M. C.: Mineral dust aerosols over the Sahara: meteorological controls on emission and transport and implications for modeling, Reviews of Geophysics, 50, RG1007, doi:10.1029/2011RG000362, 2012.

Kok, J. F.: A scaling theory for the size distribution of emitted dust aerosols suggests climate models underestimate the size of the global dust cycle, Proceedings of the National Academy of Sciences of the United States of America, 108, 1016–1021, doi:10.1073/pnas.1014798108, 2011.

Krzic, A., Tosic, I., Djurdjevic, V., Veljovic, K., and Rajkovic, B.: Changes in climate indices for Serbia according to the SRES-A1B and SRES-A2 scenarios, Climate Research, 49, 73–86, doi:10.3354/cr01008, 2011.

Lamarque, J.-F., Bond, T. C., Eyring, V., Granier, C., Heil, A., Klimont, Z., Lee, D., Liousse, C., Mieville, A., Owen, B., Schultz, M. G., Shindell, D., Smith, S. J., Stehfest, E., Aardenne, J. V., Cooper, O. R., Kainuma, M., Mahowald, N., McConnell, J. R., Naik, V., Riahi, K., and van Vuuren, D. P.: Historical (1850–2000) gridded anthropogenic and biomass burning emissions of reactive gases and aerosols: methodology and application, Atmospheric, Chemistry and Physics, 10, 7017–7039, doi:10.5194/acp-10-7017-2010, 2010.

Lamarque, J.-F., Shindell, D. T., Josse, B., Young, P. J., Cionni, I., Eyring, V., Bergmann, D., Cameron-Smith, P., Collins, W. J., Doherty, R., Dalsoren, S., Faluvegi, G., Folberth, G., Ghan, S. J., Horowitz, L., Lee, Y. H., MacKenzie, I. A., Nagashima, T., Naik, V., Plummer, D., Righi, M., Rumbold, S. T., Schulz, M., Skeie, R. B., Stevenson, D. S., Strode, S., Sudo, K., Szopa, S., Voulgarakis, A., and Zeng, G.: The Atmospheric Chemistry and Climate Model Intercomparison Project (ACCMIP): overview and description of models, simulations and climate diagnostics, Geoscientific Model Development, 6, 179–206, doi:10.5194/gmd-6-179-2013, 2013.

Lelieveld, J., Berresheim, H., Borrmann, S., Crutzen, P. J., Dentener, F. J., Fischer, H., Feichter, J., Flatau, P. J., Heland, J., Holzinger, R., Korrmann, R., Lawrence, M. G., Levin, Z., Markowicz, K. M., Mihalopoulos, N., Minikin, A., Ramanathan, V., de Reus, M., Roelofs, G. J., Scheeren, H. A., Sciare, J., Schlager, H., Schultz, M., Siegmund, P., Steil, B., Stephanou, E. G., Stier, P., Traub, M., Warneke, C., Williams, J., and Ziereis, H.: Global Air Pollution Crossroads over the Mediterranean, Science, 298, 794–799, doi:10.1126/science.1075457, 2002.

Levy, R. C., Remer, L. A., Mattoo, S., Vermote, E. F., and Kaufman, Y. J.: Second-generation operational algorithm: Retrieval of aerosol properties over land from inversion of Moderate Resolution Imaging Spectroradiometer spectral reflectance, Journal of Geophysical Research, 112, D13 211, doi:10.1029/2006JD007811, 2007.

Levy, R. C., Remer, L. A., Kleidman, R. G., Mattoo, S., Ichoku, C., Kahn, R., and Eck, T. F.: Global evaluation of the collection 5 modis dark-target aerosol products over land, Atmospherics, Chemistry and Physics, 10, 10 399–10 420, doi:10.5194/acp-10-10399-2010, 2010.

Lucas-Picher, P., Somot, S., Déqué, M., Decharme, B., and Alias, A.: Evaluation of the regional climate model ALADIN to simulate the climate over North America in the CORDEX framework, Climate Dynamics, 41, 1117–1137, doi:10.1007/s00382-012-1613-8, 2013.

Léon, J.-F., Augustin, P., Mallet, M., Pont, V., Dulac, F., Fourmentin, M., and Lambert, D.: Aerosol vertical distribution, optical properties and transport over Corsica (Western Mediterranean), Atmospheric Chemistry and Physics, this issue, in prep.

L'Hévéder, B., Li, L., Sevault, F., and Somot, S.: Interannual variability of deep convection in the Northwestern Mediterranean simulated with a coupled AORCM, Climate Dynamics, pp. 1–24, doi:10.1007/s00382-012-1527-5, 2012.

Mahowald, N., Albani, S., Kok, J. F., Engelstaeder, S., Scanza, R., Ward, D. S., and Flanner, M. G.: The size distribution of desert dust aerosols and its impact on the Earth system, Aeolian Research, 15, 53–71, doi:10.1016/j.aeolia.2013.09.002, 2013.

Mariotti, A. and Dell'Aquila, A.: Decadal climate variability in the Mediterranean region: roles of large-scale forcings and regional processes, Climate Dynamics, 38, 1129–1145, doi:10.1007/s00382-011-1056-7, 2012.

Marticorena, B. and Bergametti, G.: Modeling the atmosphere dust cycle: 1. Design of a soil-derived dust emission scheme, Journal of Geophysical Research, 100, 16,415–16,430, 1995.

Masson, V., Champeaux, J., Chauvin, F., Meriguet, C., and Lacaze, R.: A global database of land surface parameters at 1-km resolution in meteorological and climate models, Journal of Climate, 16, 1261–1282, 2003.

Meier, J., Tegen, I., Heinold, B., and Wolke, R.: Direct and semi-direct radiative effects of absorbing aerosols in Europe: Results from a regional model, Geophysical Research Letters, 39, L09 802, doi:10.1029/2012GL050994, 2012.

Michou, M., Nabat, P., and Saint-Martin, D.: Development and basic evaluation of a prognostic aerosol scheme in the CNRM Climate Model, Geoscientific Model Developments Discussion, 7, 1–63, doi:10.5194/gmdd-7-1-2014, 2014.

Middleton, N. J. and Goudie, A. S.: Saharan dust: sources and trajectories, Transactions of the Institute of British Geographers, 26, 165–181, doi:10.1111/1475-5661.00013, 2001.

Mlawer, E. J., Taubman, S. J., Brown, P. D., Iacono, M. J., and Clough, S. A.: Radiative transfer for inhomogeneous atmospheres: RRTM, a validated correlated-k model for the longwave, Journal of Geophysical Research, 102, 16 663–16 682, 1997.

Morcrette, J.-J.: Description of the Radiation Scheme in the ECMWF Model, Tech. rep., ECMWF, 1989.

Morcrette, J.-J., Boucher, O., Jones, L., Salmond, D., Bechtold, P., Beljaars, A., Benedetti, A., Bonet, A., Kaiser, J. W., Razinger, M., Schulz, M., Serrar, S., Simmons, J., Sofiev, M., Suttie, M., Tompkins, A. M., and Untch, A.: Aerosol analysis and forecast in the european centre for medium-range weather forecasts integrated forecast system: Forward modeling, Journal of Geophysical Research, 114, D06 206, doi:10.1029/2008JD011235, 2009.

Moulin, C., Guillard, F., Dulac, F., and Lambert, C. E.: Long-term daily monitoring of Saharan dust load over ocean using Meteosat ISCCP-B2 data 1. Methodology and preliminary results for 1983-1994 in the Mediterranean, Journal of Geophysical Research, 102, 16,947–16,958, 1997.

Moulin, C., Lambert, C. E., Dayan, U., Masson, V., Ramonet, M., Bousquet, P., Legrand, M., Balkanski, Y. J., Guelle, W., Marticorena, B., Bergametti, G., and Dulac, F.: Satellite climatology of African dust transport in the Mediterranean atmosphere, Journal of Geophysical Research, 103, 13,137–13,144, doi:10.1029/98JD00171, 1998.

Nabat, P., Solmon, F., Mallet, M., Kok, J. F., and Somot, S.: Dust emission size distribution impact on aerosol budget and radiative forcing over the Mediterranean region: a regional climate model approach, Atmospheric, Chemistry and Physics, 12, 10 545–10 567, doi:10.5194/acp-12-10545-2012, 2012.

Nabat, P., Somot, S., Mallet, M., Chiapello, I., Morcrette, J. J., Solmon, F., Szopa, S., Dulac, F., Collins, W., Ghan, S., Horowitz, L. W., Lamarque, J. F., Lee, Y. H., Naik, V., Nagashima, T., Shindell, D., and Skeie, R.: A 4-D climatology (1979–2009) of the monthly tropospheric aerosol optical depth distribution over the Mediterranean region from a comparative evaluation and blending of remote sensing and model products, Atmospheric Measurement Techniques, 6, 1287–1314, doi:10.5194/amt-6-1287-2013, 2013.

Nabat, P., Somot, S., Mallet, M., Sevault, F., Chiacchio, M., and Wild, M.: Direct and semi-direct aerosol radiative effect on the Mediterranean climate variability using a Regional Climate System Model, Climate Dynamics, in press, doi:10.1007/s00382-014-2205-6, 2014.

Noilhan, J. and Mahfouf, J.-F.: The ISBA land surface parameterisation scheme, Global and Planetary Change, 13, 145–159, doi:10.1016/0921-8181(95)00043-7, 1996.

Papadimas, C. D., Hatzianastassiou, N., Mihalopoulos, N., Querol, X., and Vardavas, I.: Spatial and temporal variability in aerosol properties over the Mediterranean basin based on 6-year (2000–2006) MODIS data, Journal of Geophysical Research, 113, D11 205, doi:10.1029/2007JD009189, 2008.

Pappalardo, G., Amodeo, A., Apituley, A., Comeron, A., Freudenthaler, V., Linne, H., Ansmann, A., Bösenberg, J., D'Amico, G., Mattis, I., Mona, L., Wandinger, U., Amiridis, V., Alados-Arboledas, L., Nicolae, D., and Wiegner, M.: EARLINET: towards an advanced sustainable European aerosol lidar network, Atmospheric Measurement Techniques Discussions, 7, 2929–2980, doi:10.5194/amtd-7-2929-2014, 2014.

Quaas, J., Ming, Y., Menon, S., Takemura, T., Wang, M., Penner, J. E., Gettelman, A., Lohmann, U., Bellouin, N., Boucher, O., Sayer, A. M., Thomas, G. E., McComiskey, A., Feingold, G., Hoose, C., Kristjánsson, J. E., Liu, X., Balkanski, Y., Donner, L. J., Ginoux, P. A., Stier, P., Grandey, B., Feichter, J., Sednev, I., Bauer, S. E., Koch, D., Grainger, R. G., Kirkevag, A., Iversen, T., Seland, O., Easter, R., Ghan, S. J., Rasch, P. J., Morrison, H., Lamarque, J.-F., Iacono, M. J., Kinne, S., and Schulz, M.: Aerosol indirect effects – general circulation model intercomparison and evaluation with satellite data, Atmospheric Chemistry and Physics, 9, 8697–8717, doi:10.5194/acp-9-8697-2009, 2009.

Radu, R., Déqué, M., and Somot, S.: Spectral nudging in a spectral regional climate model, Tellus, 60A, 898–910, doi:10.1111/j.1600-0870.2008.00341.x, 2008.

Reba, M. N. M., Rocadenbosch, F., Sicard, M., Kumar, D., and Tomás, S.: On the lidar ratio estimation from the synergy between AERONET sun-photometer data and elastic lidar inversion, Proc. of the 25th International Laser Radar Conference, ISBN 978-5-94458-109-9, Saint-Petersburg (Rusia), 5–9 July 2010, p. 1102–1105, 2010.

Santese, M., Perrone, M. R., Zakey, A. S., Tomasi, F. D., and Giorgi, F.: Modeling of Saharan dust outbreaks over the Mediterranean by RegCM3: case studies, Atmospheric, Chemistry and Physics, 10, 133–156, 2010.

Schulz, M., de Leeuw, G., and Balkanski, Y.: Sea-salt aerosol source functions and emissions in [Emission of Atmospheric Trace Compounds], Kluwer Acad., Norwell, Mass., c. granier, p. artaxo, and c. e. reeves edn., 2004.

Schulz, M., Textor, C., Kinne, S., Balkanski, Y., Bauer, S., Berntsen, T., Berglen, T., Boucher, O., Dentener, F., Guibert, S., Isaksen, I. S. A., Iversen, T., Koch, D., Kirkevag, A., Liu, X., Montanaro, V., Myhre, G., Penner, J. E., Pitari, G., Reddy, S., Seland, O., Stier, P., and Takemura, T.: Radiative forcing by aerosols as derived from the AeroCom present-day and preindustrial simulations, Atmospheric Chemistry and Physics, 6, 5225–5246, doi:10.5194/acp-6-5225-2006, 2006.

Somot, S., Sevault, F., Déqué, M., and Crépon, M.: 21st century climate change scenario for the Mediterranean using a coupled atmosphere–ocean regional climate model, Global and Planetary Change, 63, 112–126, doi:10.1016/j.gloplacha.2007.10.003,

2008.

Spyrou, C., Kallos, G., Mitsakou, C., Athanasiadis, P., Kalogeri, C., and Iacono, M.: Modeling the radiative effects of desert dust on weather and regional climate, Atmospheric Chemistry and Physics, 13, 5489–5504, doi:10.5194/acp-13-5489-2013, 2013.

Tanré, D., Geleyn, J., and Slingo, J.: First results of an advanced aerosol-radiation interaction in ECMWF low resolution global model, H. E. Gerber and A. Deepak, a. deepak edn., 1984.

Tanré, D., Kaufman, Y. J., Herman, M., and Mattoo, S.: Remote sensing of aerosol properties over oceans using the MODIS/EOS spectral radiances, Journal of Geophysical Research, 102, 16,971–16,988, 1997.

Taylor, K. E.: Summarizing multiple aspects of model performance in a single diagram, Journal of Geophysical Research, 106, 7183–7192, doi:10.1029/2000JD900719, 2001.

Tegen, I., Hollrig, P., Chin, M., Fung, I., Jacob, D., and Penner, J.: Contribution of different aerosol species to the global aerosol extinction optical thickness: Estimates from model results, Journal of Geophysical Research, 102, 23,895–23,915, 1997.

Tesche, M., Ansmann, A., Müller, D., Althausen, D., Mattis, I., Heese, B., Freundenthaler, V., Wiegner, M., Esselborn, M., Pisani, G., and Knippertz, P.: Vertical profiling of Saharan dust with Raman lidars and airborne HSRL in southern Morocco during SAMUM, Tellus B, 61, 144–164, doi:10.1111/j.1600-0889.2008.00390.x, 2009.

Textor, C., Schulz, M., Guibert, S., Kinne, S., Balkanski1, Y., Bauer, S., Berntsen, T., Berglen, T., Boucher, O., Chin, M., Dentener, F., Diehl, T., Easter, R., Feichter, H., Fillmore, D., Ghan, S., Ginoux, P., Gong, S., Grini, A., Hendricks, J., Horowitz, L., Huang, P., Isaksen, I., Iversen, T., Kloster, S., Koch, D., Kirkev, A., Kristjansson, J. E., Krol, M., Lauer, A., Lamarque, J. F., Liu, X., Montanaro, V., Myhre, G., Penner, J., Pitari, G., Reddy, S., Seland, O., Stier, P., Takemura, T., and Tie, X.: Analysis and quantification of the diversities of aerosol life cycles within AeroCom, Atmosphery, Chemistry and Physics, 6, 1777–1813, 2006.

Todd, M. C., Karam, D. B., Cavazos, C., Bouet, C., Heinold, B., Baldasano, J. M., Cautenet, G., Koren, I., Perez, C., Solmon, F., Tegen, I., Tulet, P., Washington, R., and Zakey, A.: Quantifying uncertainty in estimates of mineral dust flux: An intercomparison of model performance over the Bodélé Depression, northern Chad, Journal of Geophysical Research, 113, D24 107, doi:10.1029/2008JD010476, 2008.

Turuncoglu, U. U., Giuliani, G., Elguindi, N., and Giorgi, F.: Modelling the Caspian Sea and its catchment area using a coupled regional atmosphere-ocean model (RegCM4-ROMS): model design and preliminary results, Geoscientific Model Development, 6, 283–299, doi:10.5194/gmd-6-283-2013, 2013.

Valcke, S.: The OASIS3 coupler : a European climate modelling community software, Geoscientific Model Development, 6, 373–388, doi:10.5194/gmd-6-373-2013, 2013.

Vogel, B., Vogel, H., Bümer, D., Bangert, M., Lundgren, K., Rinke, R., and Stanelle, T.: The comprehensive model system COSMO-ART – Radiative impact of aerosol on the state of the atmosphere on the regional scale, Atmospheric Chemistry and Physics, 9, 8661–8680, doi:10.5194/acp-9-8661-2009, 2009.

Woodage, M. J., Slingo, A., Woodward, S., and Comer, R. E.: Simulations of Desert Dust and Biomass Burning Aerosols with a High-Resolution Atmospheric GCM, Journal of Climate, 23(7), 1636–1659, doi:10.1175/2009JCLI2994.1, 2010.

Zanis, P.: A study on the direct effect of anthropogenic aerosols on near surface air temperature over Southeastern Europe during summer 2000 based on regional climate modeling, Annales Geophysicae, 27, 3977–3988, 2009.

Zanis, P., Ntogras, C., Zakey, A., Pytharoulis, I., and Karacostas, T.: Regional climate feedback of anthropogenic aerosols over Europe using RegCM3, Climate research, 52, 267–278, doi:10.3354/cr01070, 2012.